

# You Can't Get Through Szekeres Wormholes or Regularity, Topology and Causality in Quasi-Spherical Szekeres Models

Charles Hellaby <sup>\*</sup>

Department of Mathematics and Applied Mathematics,  
University of Cape Town, Rondebosch 7701, South Africa  
cwh@maths.uct.ac.za

and

Andrzej Krasiński <sup>†</sup>

N. Copernicus Astronomical Center, Polish Academy of Sciences,  
Bartycka 18, 00 716 Warszawa, Poland  
akr@camk.edu.pl

## Abstract

The spherically symmetric dust model of Lemaître-Tolman can describe wormholes, but the causal communication between the two asymptotic regions through the neck is even less than in the vacuum (Schwarzschild-Kruskal-Szekeres) case. We investigate the anisotropic generalisation of the wormhole topology in the Szekeres model. The function  $E(r, p, q)$  describes the deviation from spherical symmetry if  $\partial_r E \neq 0$ , but this requires the mass to be increasing with radius,  $\partial_r M > 0$ , i.e. non-zero density. We investigate the geometrical relations between the mass dipole and the locii of apparent horizon and of shell-crossings. We present the various conditions that ensure physically reasonable quasi-spherical models, including a regular origin, regular maxima and minima in the spatial sections, and the absence of shell-crossings. We show that physically reasonable values of  $\partial_r E \neq 0$  cannot compensate for the effects of  $\partial_r M > 0$  in any direction, so that communication through the neck is still worse than the vacuum.

We also show that a handle topology cannot be created by identifying hypersurfaces in the two asymptotic regions on either side of a wormhole, unless a surface layer is allowed at the junction. This impossibility includes the Schwarzschild-Kruskal-Szekeres case.

## PACS:

04.20.Gz, spacetime topology & causal structure

04.40.Nr, spacetimes with fluids or fields

04.70.Bw, classical black holes

---

<sup>\*</sup>This research was supported by a grant from the South African National Research Foundation,  
<sup>†</sup>and by the Polish Research Committee grant no 2 P03B 060 17.

Keywords: Szekeres metric, shell crossings, topology, wormholes, causal structure, apparent horizon

Short title: Wormholes and Other Quasi-Spherical Szekeres Models

Submitted to: Physical Review D, June 2002

gr-qc/0206052

# 1 Introduction

The Szekeres metric is a dust model, which has no Killing vectors [6], but contains the Lemaître-Tolman (LT) model as the spherically symmetric special case, which itself contains the Schwarzschild-Kruskal-Szekeres [18, 23] manifold as the vacuum case. As with the LT model, it is written in synchronous coordinates, and the particles of dust are comoving. The constant time slices are foliated by 2-surfaces of constant coordinate  $r$ , which have 2-metrics of spheres, planes or pseudo-spheres, depending on the value of parameter  $\epsilon$ . See [17] for a review of its known properties.

Despite the inhomogeneity of the model, and the lack of Killing vectors, any surface of constant coordinate ‘radius’  $r$  in the  $\epsilon = +1$  case can be matched onto a Schwarzschild vacuum metric [3, 4], and any surface of constant time  $t$  is conformally flat [2].

We here investigate the topological and causal properties of the quasi-spherical case,  $\epsilon = +1$ , subject to the requirements for a physically reasonable model. Reasonability requirements include, well behaved metric components, non-divergent density and curvature, regular spherical origins, regular maxima and minima in the spatial sections, and prohibition of shell crossings. Choosing well behaved coordinates also assists in avoiding the confusion of coordinate singularities.

Studying such models of low symmetry is important, so that one can check which properties of spherically symmetric investigations of cosmology and gravitational collapse are preserved, and which are not.

The subjects studied in this paper in some detail are the following:

1. The dipole-like variation of mass-density; the locus of its poles and of the equator, and the images of the equator under the Riemann projection.
2. Conditions for regularity of the geometry at the origin  $R = 0$ .
3. Intersections of the shell crossings with the surfaces of constant  $(t, r)$ , and conditions for avoidance of shell crossings.
4. Conditions for regular maxima and minima at a neck.
5. Conditions for a handle topology of a  $t = \text{const}$  space, and the impossibility of preserving this topology during evolution of the model.
6. Apparent horizons – their shape, intersections with the surfaces of constant  $(t, r)$ , relations between these intersections and those of shell crossings, and with the dipole equator, location of an AH with respect to the  $R = 2M$  hypersurface, the intersection of an AH with a neck.
7. The impossibility of sending a light ray through the neck so that it would emerge from

under the AH on the other side.

8. Numerical examples of light paths traversing the neck and of those going in its vicinity.

## 2 The Szekeres Metric

The LT-type Szekeres metric [24] is<sup>1</sup>:

$$ds^2 = -dt^2 + \frac{(R' - R \frac{E'}{E})^2}{(\epsilon + f)} dr^2 + R^2 \frac{(dp^2 + dq^2)}{E^2}, \quad (1)$$

where  $' \equiv \partial/\partial r$ ,  $\epsilon = \pm 1, 0$  and  $f = f(r) \geq -\epsilon$  is an arbitrary function of  $r$ .

The function  $E$  is given by

$$E(r, p, q) = A(p^2 + q^2) + 2B_1p + 2B_2q + C, \quad (2)$$

where functions  $A = A(r)$ ,  $B_1 = B_1(r)$ ,  $B_2 = B_2(r)$ , and  $C = C(r)$  satisfy the relation

$$4(AC - B_1^2 - B_2^2) = \epsilon, \quad \epsilon = 0, \pm 1, \quad (3)$$

but are otherwise arbitrary.

The function  $R = R(t, r)$  satisfies the Friedmann equation for dust

$$\dot{R}^2 = \frac{2M}{R} + f, \quad (4)$$

where  $\dot{\cdot} \equiv \partial/\partial t$  and  $M = M(r)$  is another arbitrary function of coordinate “radius”,  $r$ . It follows that the acceleration of  $R$  is always negative

$$\ddot{R} = \frac{-M}{R^2}. \quad (5)$$

Here  $M(r)$  plays the role of an effective gravitational mass for particles at comoving “radius”  $r$ . For  $\epsilon = +1$ , it is simply the total gravitational mass within the sphere of radius  $r$ . We assume  $M \geq 0$  and  $R \geq 0$ . In (4)  $f(r)$  represents twice the energy per unit mass of the particles in the shells of matter at constant  $r$ , but in the metric (1) it also determines the geometry of the spatial sections  $t = \text{constant}$  (c.f. [10]). The evolution of  $R$  depends on the value of  $f$ ; it can be:

hyperbolic,  $f > 0$ :

$$R = \frac{M}{f} (\cosh \eta - 1), \quad (6)$$

$$(\sinh \eta - \eta) = \frac{f^{3/2} \sigma(t - a)}{M}, \quad (7)$$

---

<sup>1</sup>The results presented in Ref. [24] contain a few misleading typos that were corrected in Ref. [7]. The notation used here does not follow the traditional one

parabolic,  $f = 0$ :

$$R = M \frac{\eta^2}{2}, \quad (8)$$

$$\frac{\eta^3}{6} = \frac{\sigma(t-a)}{M}, \quad (9)$$

$$\text{i.e. } R = \left( \frac{9M(t-a)^2}{2} \right)^{1/3}, \quad (10)$$

elliptic,  $f < 0$ :

$$R = \frac{M}{(-f)} (1 - \cos \eta), \quad (11)$$

$$(\eta - \sin \eta) = \frac{(-f)^{3/2} \sigma(t-a)}{M}, \quad (12)$$

where  $a = a(r)$  is the last arbitrary function, giving the local time of the big bang or crunch  $R = 0$  and  $\sigma = \pm 1$  permits time reversal. More correctly, the three types of evolution hold for  $f/M^{2/3} >, =, < 0$ , since  $f = 0$  at a spherical type origin for all 3 evolution types. The behaviour of  $R(t, r)$  is identical to that in the LT model, and is unaffected by  $(p, q)$  variations.

A more meaningful way to write  $E$  is

$$E(r, p, q) = \frac{S}{2} \left\{ \left( \frac{p - P}{S} \right)^2 + \left( \frac{q - Q}{S} \right)^2 + \epsilon \right\}, \quad (13)$$

where  $S = S(r)$ ,  $P = P(r)$ , and  $Q = Q(r)$  are arbitrary functions, and

$$A = \frac{1}{2S}, \quad B_1 = \frac{-P}{2S}, \quad B_2 = \frac{-Q}{2S}, \quad C = \frac{P^2 + Q^2 + \epsilon S^2}{2S}. \quad (14)$$

The metric component

$$\frac{(dp^2 + dq^2)}{E^2} \quad (15)$$

is actually the unit sphere, plane, pseudo-sphere in Riemann projection:

$$\epsilon = +1 \quad \frac{(p - P)}{S} = \cot \left( \frac{\theta}{2} \right) \cos(\phi), \quad \frac{(q - Q)}{S} = \cot \left( \frac{\theta}{2} \right) \sin(\phi), \quad (16)$$

$$\epsilon = 0 \quad \frac{(p - P)}{S} = \left( \frac{2}{\theta} \right) \cos(\phi), \quad \frac{(q - Q)}{S} = \left( \frac{2}{\theta} \right) \sin(\phi), \quad (17)$$

$$\epsilon = -1 \quad \frac{(p - P)}{S} = \coth \left( \frac{\theta}{2} \right) \cos(\phi), \quad \frac{(q - Q)}{S} = \coth \left( \frac{\theta}{2} \right) \sin(\phi). \quad (18)$$

It seems reasonable to expect  $S > 0$ , but it is not obviously impossible for  $S$  to reach or pass through zero.

The factor  $\epsilon$  determines whether the  $p$ - $q$  2-surfaces are spherical ( $\epsilon = +1$ ), pseudo-spherical ( $\epsilon = -1$ ), or planar ( $\epsilon = 0$ ). In other words, it determines how the constant  $r$  2-surfaces foliate

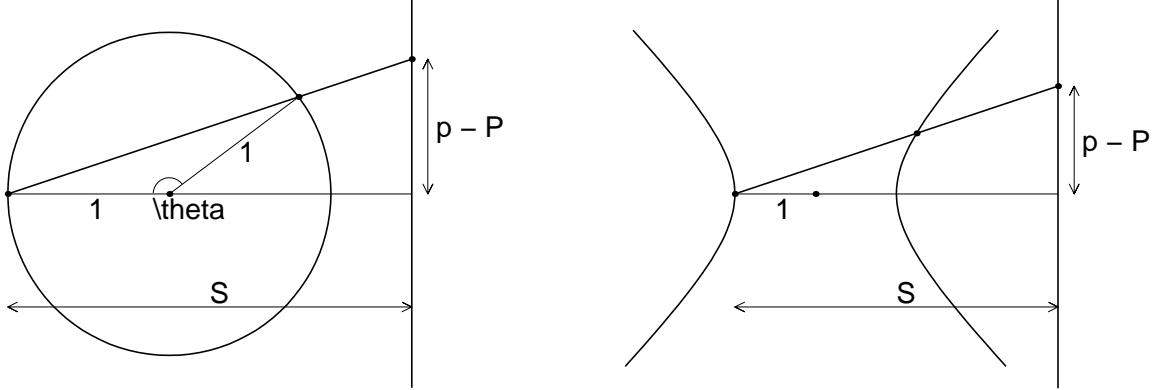


Figure 1: The Riemann projection from  $(\theta, \phi)$  to  $(p, q)$  coordinates for spheres & hyperbolae. The diagrams show only the  $\phi = 0, \pi$  section, i.e. the  $q = Q$  section.

the 3-d spatial sections of constant  $t$ . The function  $E$  determines how the coordinates  $(p, q)$  map onto the unit 2-sphere (plane, pseudo-sphere) at each value of  $r$ . At each  $r$  these 2-surfaces are multiplied by the areal ‘‘radius’’  $R = R(t, r)$  that evolves with time. Thus the  $r$ - $p$ - $q$  3-surfaces are constructed out of a sequence of 2-dimensional spheres (pseudo-spheres, planes) that are not concentric, since the metric component  $g_{rr}$  depends on  $p$  and  $q$  as well as  $r$  and  $t$ .

The  $(p, q)$ -coordinates in the cases  $\epsilon = +1$  and  $\epsilon = 0$  have the range  $(-\infty, +\infty)$ . In the case  $\epsilon = -1$ , the parametrization (13) does not cover the subcases  $A = 0$  and  $C = 0$  (these subcases cannot occur with  $\epsilon \geq 0$  because of (3)). Coming back to (2), we see that, for  $\epsilon = -1$  and  $A \neq 0$ ,  $E$  is zero when

$$(p + B_1/A)^2 + (q + B_2/A)^2 = 1/(4A)^2,$$

$E$  is positive for  $p$  and  $q$  outside this circle, and is negative for  $p$  and  $q$  inside it. Fig. 1 suggests that with  $\epsilon = -1$ , we should rather take  $(-E)$  as the metric function so that  $p$  and  $q$  have finite rather than semi-infinite ranges. However, both the  $E > 0$  and  $E < 0$  regions are Szekeres spacetimes because they are mapped one onto another by

$$(p, q) = (p', q') / \sqrt{p'^2 + q'^2}, \quad (19)$$

the roles of  $A$  and  $C$  being interchanged after the transformation.

If  $A \neq 0 = C$ , then a nonzero  $C$  is restored by a translation in the  $(p, q)$  plane. If  $A = 0$ , then the metric of the  $(p, q)$ -surface is brought back to the standard Szekeres form with  $A \neq 0 \neq C$  by a Haantjes transformation (a conformal symmetry transformation of a flat space, see [16] for a description) in the  $(p, q)$  surface, which also restores the appropriate form of  $g_{rr}$ .

The surface area of a  $(t = \text{const}, r = \text{const})$  surface is finite only in the  $\epsilon = +1$  case, where it equals  $4\pi R^2$ . In the other two cases, it is infinite.

The 6 arbitrary functions  $f$ ,  $M$ ,  $a$ ,  $P$ ,  $Q$  and  $S$  represent 5 physical freedoms to control the inhomogeneity, plus a coordinate freedom to rescale  $r$ .

The density and the Kretschmann scalar are functions of all four coordinates

$$8\pi\rho = G_{tt} = \frac{2(M' - 3ME'/E)}{R^2(R' - RE'/E)}, \quad (20)$$

$$\mathcal{K} = R^{\alpha\beta\gamma\delta}R_{\alpha\beta\gamma\delta} = (8\pi)^2 \left[ \frac{4}{3}\bar{\rho}^2 - \frac{8}{3}\bar{\rho}\rho + 3\rho^2 \right], \quad (21)$$

where

$$8\pi\bar{\rho} = \frac{6M}{R^3} \quad (22)$$

is the mean density within "radius"  $r$ . For all  $\rho$  and  $\bar{\rho}$  we have  $\mathcal{K} \geq 0$ , but assumptions of positive mass and density require  $\rho \geq 0$  and  $\bar{\rho} \geq 0$ . Clearly there are density and curvature singularities at  $R = 0$  — the bang and/or crunch — and at  $R' = RE'/E$ ,  $M' \neq 3ME'/E$  — shell crossings. Additionally,  $\rho$  but not  $\mathcal{K}$  passes through zero where  $E'/E$  exceeds  $M'/3M$ .

The matter flow  $u^\alpha = \delta_t^\alpha$ , with projection tensor  $h_{\alpha\beta} = g_{\alpha\beta} + u_\alpha u_\beta$ , has the following properties, which are almost trivial to calculate with GRTensor [20]:

$$\Theta = \nabla_\alpha u^\alpha = \frac{(\dot{R}' - 3\dot{R}E'/E + 2R'\dot{R}/R)}{(R' - RE'/E)}, \quad (23)$$

$$A^\alpha = u^\beta \nabla_\beta u^\alpha = 0, \quad (24)$$

$$\sigma^\alpha_\beta = g^{\alpha\gamma}(\nabla_{(\gamma} u_{\alpha)} + u_{(\gamma} A_{\alpha)}) - \frac{\Theta}{3} h^\alpha_\beta = \frac{(\dot{R}' - R'\dot{R}/R)}{3(R' - RE'/E)} \text{diag}(0, 2, -1, -1), \quad (25)$$

$$\omega_{\alpha\beta} = \nabla_{[\beta} u_{\alpha]} + u_{[\beta} A_{\alpha]} = 0, \quad (26)$$

$$E^\alpha_\beta = C^\alpha_{\gamma\beta\delta} u^\gamma u^\delta = \frac{M(R' - RM'/3M)}{R^3(R' - RE'/E)} \text{diag}(0, -2, 1, 1), \quad (27)$$

$$H_{\alpha\beta} = \frac{1}{2} \epsilon_{\alpha\gamma\mu\nu} C^{\mu\nu}{}_{\beta\delta} u^\gamma u^\delta = 0. \quad (28)$$

Note that the relation between the active gravitational mass  $M$  and the "sum-of-rest-masses"  $\mathcal{M}$  is the same in the  $\epsilon = +1$  Szekeres model as in the LT model:

$$\mathcal{M}' = M'/\sqrt{1+f}. \quad (29)$$

The sum of the rest masses contained inside the sphere of coordinate radius  $r$  at the time  $t$  is defined by:

$$\mathcal{M} = \int \rho \sqrt{|g_3|} d_3x, \quad (30)$$

where  $g_3$  is the determinant of the metric of the  $t = \text{const}$  hypersurface, and the integral is taken with respect to the variables  $p$  and  $q$  from  $-\infty$  to  $+\infty$ , and with respect to  $r$  from  $r_0$  at the origin to the current value  $r$ . We have

$$\sqrt{|g_3|} = \frac{E}{\sqrt{1+f}} (R/E)^2 (R/E)'. \quad (31)$$

Consequently

$$\mathcal{M} = \frac{1}{4\pi} \int_{-\infty}^{+\infty} dq \int_{-\infty}^{+\infty} dp \int_{r_0}^r dx \left[ \frac{E}{\sqrt{1+f}} (M/E^3)' \right] (t, p, q, x). \quad (32)$$

The term containing  $E'$  is integrated by parts with respect to  $x$  in order to move the prime (which, in the integrand, means  $\frac{\partial}{\partial x}$ ) away from  $E$  to functions that do not depend on  $p$  and  $q$ . The result is

$$\begin{aligned} \mathcal{M} = & \frac{3}{2} \left[ \frac{M}{\sqrt{1+f}}(r) - \frac{M}{\sqrt{1+f}}(r_0) \right] \cdot \frac{1}{4\pi} \int_{-\infty}^{+\infty} dq \int_{-\infty}^{+\infty} dp E^{-2} \\ & + \frac{1}{8\pi} \int_{-\infty}^{+\infty} dq \int_{-\infty}^{+\infty} dp \int_{r_0}^r dx E^{-2} \left[ \frac{3Mf'}{2(1+f)^{3/2}} - \frac{M'}{\sqrt{1+f}} \right]. \end{aligned} \quad (33)$$

We note that

$$\int_{-\infty}^{+\infty} dq \int_{-\infty}^{+\infty} dp E^{-2} = 4\pi \quad (34)$$

(this is the surface area of a unit sphere), and so

$$\mathcal{M} = \frac{3}{2} \left[ \frac{M}{\sqrt{1+f}}(r) - \frac{M}{\sqrt{1+f}}(r_0) \right] + \frac{1}{2} \int_{r_0}^r \left[ \frac{3Mf'}{2(1+f)^{3/2}} - \frac{M'}{\sqrt{1+f}} \right] dx. \quad (35)$$

From here, we obtain the same relation that holds in the L-T model, (29).

Note that this result holds only in the  $\epsilon = +1$  Szekeres model (the spherical one). With  $\epsilon = 0$  or  $\epsilon = -1$ , the total surface area of the  $(p, q)$ -surface is infinite, and so  $\mathcal{M}$  cannot be defined.

## 2.1 Special Cases and Limits

The Lemaître-Tolman (LT) model is the spherically symmetric special case  $\epsilon = +1$ ,  $E' = 0$ .

The vacuum case is  $(M' - 3ME'/E) = 0$  which gives  $M \propto E^3$ , and this requires

$$M' = 0 = S' = P' = Q' = E' \quad (36)$$

and any region over which this holds is the Schwarzschild metric in LT coordinates [10], with mass  $M$ . (See [12] for the full transformation in the general case.)

In the null limit,  $f \rightarrow \infty$ , in which the ‘dust’ particles move at light speed [11, 5], the metric becomes a pure radiation Robinson-Trautman metric of Petrov type D, as given in Exact Solutions [15], equation (24.60) with (24.62)<sup>2</sup> The Kinnersley rocket [14] is the  $\epsilon = +1$  case of this null limit, which is actually more general than the axially symmetric form given in [11].

The KS-type Szkeres metric was shown in [11] to be special case of the above LT-type metric, under a suitable limit.

---

<sup>2</sup>Ref [5] corrected ref [11]’s mistaken claim that the null limit of Szekeres was a new metric.

## 2.2 Basic Physical Restrictions

1. For a metric of Lorentzian signature  $(- +++)$ , we require

$$\epsilon + f \geq 0 \quad (37)$$

with equality only occurring where  $(R' - RE'/E)^2/(\epsilon + f) > 0$ . Clearly, pseudo-spherical foliations,  $\epsilon = -1$ , require  $f \geq 1$ , and so are only possible for hyperbolic spatial sections,  $f > 0$ . Similarly, planar foliations,  $\epsilon = 0$ , are only possible for parabolic or hyperbolic spatial sections,  $f \geq 0$ , whereas spherical foliations are possible for all  $f \geq -1$ .

2. We obviously choose the areal radius  $R$  to be positive,

$$R \geq 0 \quad (38)$$

( $R = 0$  is either an origin, or the bang or crunch. In no case is a continuation to negative  $R$  possible.)

3. The mass  $M(r)$  must be positive, so that any vacuum exterior has positive Schwarzschild mass,

$$M \geq 0. \quad (39)$$

4. We require the metric to be non degenerate & non singular, except at the bang or crunch. Since  $(dp^2 + dq^2)/E^2$  maps to the unit sphere, plane or pseudo-sphere,  $|S(r)| \neq 0$  is needed for a sensible mapping, and so  $S > 0$  is a reasonable choice. In the cases  $\epsilon = 0$  or  $-1$ ,  $E$  necessarily goes to zero at certain  $(p, q)$  values where the mapping is badly behaved. For a well behaved  $r$  coordinate, we do need to specify

$$\infty > \frac{(R' - RE'/E)^2}{(\epsilon + f)} > 0, \quad (40)$$

$$\text{i.e. } (\epsilon + f) > 0 \text{ except where } (R' - RE'/E)^2 = 0. \quad (41)$$

In Lemaître-Tolman models [19, 26] ( $E' = 0$ ,  $\epsilon = 1$ ), the equality  $(1 + f) = 0 = (R')^2$  can occur in closed models where the areal radius on a spatial section is at a maximum, or in wormhole models where the areal radius is minimum,  $R'(t, r_m) = 0$ ,  $\forall t$ . These can only occur at constant  $r$  and must hold for all  $(p, q)$  values. We will consider maxima and minima again later.

5. The density must be positive, and the Kretschmann scalar must be finite, which adds

$$\text{either } M' - 3ME'/E \geq 0 \quad \text{and} \quad R' - RE'/E \geq 0 \quad (42)$$

$$\text{or } M' - 3ME'/E \leq 0 \quad \text{and} \quad R' - RE'/E \leq 0. \quad (43)$$

If  $(R' - RE'/E)$  passes through 0 anywhere other than a regular extremum, we have a shell crossing, where an inner shell of matter passes through an outer shell, and the density diverges and goes negative. This phenomenon is probably due to the spacetime coordinates being attached to the shells of matter, and is not physically realistic. Nevertheless, we would like to avoid models in which such unphysical behaviour occurs, so it is useful to find restrictions on the arbitrary functions that prevent it.

6. The various arbitrary functions should have sufficient continuity —  $C^1$  and piecewise  $C^3$  — except possibly at a spherical origin.

### 3 The Significance of $E$

#### 3.1 Properties of $E(r, p, q)$ .

Note that the Szekeres metric is covariant with the transformations  $r = g(\tilde{r})$ , where  $g$  is an arbitrary function. Hence, if  $R' < 0$  in the neighbourhood of some value  $r = r_0$ , we can take  $g = 1/\tilde{r}$  and obtain  $dR/d\tilde{r} > 0$ . Therefore,  $R' > 0$  can always be assumed to hold in some neighbourhood of any  $r = r_0$ . However, if  $R'$  changes sign somewhere, then this is a coordinate-independent property.

As seen from eq. (13), with  $\epsilon = +1$ ,  $E$  must be always nonzero. Since the sign of  $E$  is not defined by the metric, we can assume that  $E > 0$ .

Can  $E'$  change sign?

$$E' = \frac{1}{2}S' \left\{ - \left[ (p - P)^2 + (q - Q)^2 \right] / S^2 + \epsilon \right\} - \frac{1}{S} [(p - P)P' + (q - Q)Q']. \quad (44)$$

The discriminant of this with respect to  $(p - P)$  is

$$\Delta_p = \frac{1}{S^2} \left[ -\frac{S'^2}{S^2} (q - Q)^2 - 2\frac{S'}{S} (q - Q)Q' + P'^2 + \epsilon S'^2 \right]. \quad (45)$$

The discriminant of  $\Delta_p$  with respect to  $(q - Q)$  is

$$\Delta_q = 4\frac{S'^2}{S^6} (P'^2 + Q'^2 + \epsilon S'^2). \quad (46)$$

Since, with  $\epsilon = +1$ , this is never negative, the equation  $E' = 0$  will always have at least one solution (exceptional situations), and in general two. The two exceptional situations are when  $\Delta_q = 0$ . They are:

1.  $S' = 0$ . Then  $E' = 0$  has a family of solutions anyway, but the solutions define a straight line in the  $(p, q)$ -plane. This will be dealt with below (see after eq. (??)).
2.  $S' = P' = Q' = 0$ . Then  $E' \equiv 0$  at this particular value of  $r$ , and we see from eq. (20) that  $\rho$  will be spherically symmetric there. (In this case, the positions of the great circle from eq. (55) and of the poles from eq. (64) are undetermined).

When  $\Delta_q > 0$ ,  $\Delta_p$  will change sign at the following two values of  $q$ :

$$q_{1,2} = Q + \frac{S}{S'} \left( -Q' \pm \sqrt{P'^2 + Q'^2 + \epsilon S'^2} \right). \quad (47)$$

For every  $q$  such that  $q_1 < q < q_2$  there will be two values of  $p$  (and one value of  $p$  when  $q = q_1$  or  $q = q_2$ ) such that  $E' = 0$ . Those values of  $p$  are

$$p_{1,2} = P - P' \frac{S}{S'} \pm S \sqrt{ - \left( \frac{q - Q}{S} + \frac{Q'}{S'} \right)^2 + \frac{P'^2 + Q'^2}{S'^2} + \epsilon}. \quad (48)$$

The regions where  $E'$  is positive and negative depend on the sign of  $S'$ . If  $S' > 0$ , then  $E' > 0$  for  $p < p_1$  and for  $p > p_2$ , if  $S' < 0$ , then  $E' > 0$  for  $p_1 < p < p_2$ .  $E' = 0$  for  $p = p_1$  and

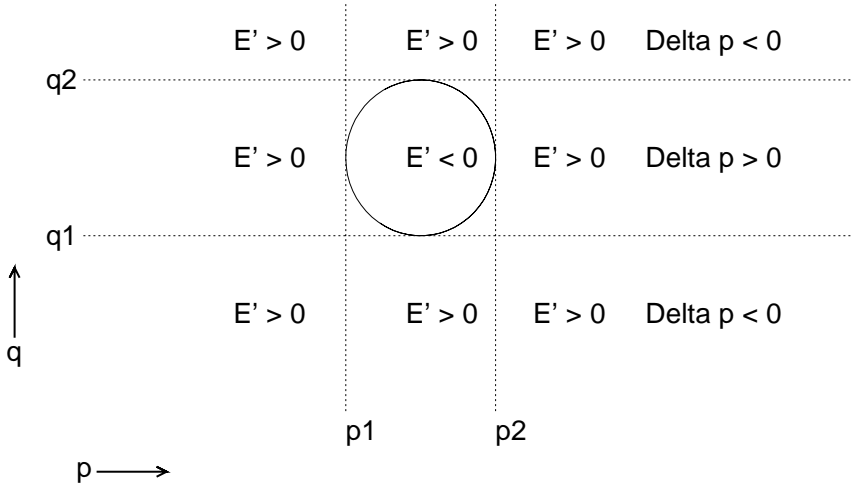


Figure 2: When  $S' > 0$ ,  $E' < 0$  inside the circle defined by (49) and  $E' > 0$  outside. Note that the  $(p, q)$  plane is a Riemann projection of a sphere, and on the sphere "inside" and "outside" are topologically equivalent.

$p = p_2$ , but note that  $p_1$  and  $p_2$  are members of a continuous family labelled by  $q$ . All the values of  $p$  and  $q$  from (47) – (48) lie on the circle

$$\left[ p - \left( P - P' \frac{S}{S'} \right) \right]^2 + \left[ q - \left( Q - Q' \frac{S}{S'} \right) \right]^2 = S^2 \left( \frac{P'^2 + Q'^2}{S'^2} + \epsilon \right). \quad (49)$$

The center of this circle is in the point

$$(p, q) = \left( P - P' \frac{S}{S'}, Q - Q' \frac{S}{S'} \right), \quad (50)$$

and the radius of this circle is

$$L_{E'} = S \sqrt{\frac{P'^2 + Q'^2}{S'^2} + \epsilon}. \quad (51)$$

The situation on the  $(p, q)$ -plane when  $S' > 0$  is shown in Fig. 2.

### 3.2 Properties of $E(r, \theta, \phi)$ .

We consider the variation of  $E(r, p, q)$  around the spheres of constant  $t$  and  $r$ .

Setting  $\epsilon = +1$  and applying the transformation (16) to (13) and to its derivative gives

$$E = \frac{S}{1 - \cos \theta}, \quad (52)$$

$$E' = -\frac{S' \cos \theta + \sin \theta (P' \cos \phi + Q' \sin \phi)}{1 - \cos \theta}, \quad (53)$$

$$\begin{aligned}
E'' &= -\frac{S'' \cos \theta + \sin \theta (P'' \cos \phi + Q'' \sin \phi)}{(1 - \cos \theta)} \\
&\quad + 2 \left( \frac{S'}{S} \right) \left( \frac{S' \cos \theta + \sin \theta (P' \cos \phi + Q' \sin \phi)}{(1 - \cos \theta)} \right) \\
&\quad + \frac{(S')^2 + (P')^2 + (Q')^2}{S}.
\end{aligned} \tag{54}$$

The locus  $E' = 0$  is

$$S' \cos \theta + P' \sin \theta \cos \phi + Q' \sin \theta \sin \phi = 0. \tag{55}$$

Writing  $z = \cos \theta$ ,  $y = \sin \theta \cos \phi$ ,  $x = \sin \theta \sin \phi$ , clearly puts  $(x, y, z)$  on a unit sphere through  $(0, 0, 0)$ , and (55) becomes  $S'z + P'x + Q'y = 0$  which is the equation of an arbitrary plane through  $(0, 0, 0)$ . Such planes all intersect the unit sphere along great circles, therefore  $E' = 0$  is a great circle, with locus

$$\tan \theta = \frac{-S'}{P' \cos \phi + Q' \sin \phi}. \tag{56}$$

The plane has unit normal  $(P', Q', S')/\sqrt{(P')^2 + (Q')^2 + (S')^2}$ .

Now it is easy to understand the meaning of the special case  $S' = 0$  mentioned after eq. (46). As seen from (56), with  $S' = 0$  we have  $\theta = 0$ , which means that the great circle defined by  $E' = 0$  passes through the pole of Riemann projection. In this case, the image of the circle  $E' = 0$  on the  $(p, q)$  plane is a straight line passing through  $(p, q) = (P, Q)$ , as indeed follows from (44). The sign of  $E'$  is different on each side of the straight line. Compare also with Figs. 4 and 5.

From (53) and (52) we find

$$\frac{E'}{E} = -\frac{S' \cos \theta + \sin \theta (P' \cos \phi + Q' \sin \phi)}{S} \tag{57}$$

thus

$$\frac{E'}{E} = \text{constant} \quad \Rightarrow \quad S'z + P'x + Q'y = S \times \text{constant} \tag{58}$$

which is a plane parallel to the  $E' = 0$  plane, implying that all loci  $E'/E = \text{constant}$  are small circles parallel to the  $E' = 0$  great circle. This will be seen to apply to shell crossings and apparent horizons.

The location of the extrema of  $E'/E$  are found as follows

$$\frac{\partial(E'/E)}{\partial \phi} = \frac{\sin \theta (P' \sin \phi - Q' \cos \phi)}{S} = 0 \quad \Rightarrow \tag{59}$$

$$\tan \phi_e = \frac{Q'}{P'} \quad \Rightarrow \quad \cos \phi_e = \epsilon_1 \frac{P'}{\sqrt{(P')^2 + (Q')^2}}, \quad \epsilon_1 = \pm 1, \tag{60}$$

$$\frac{\partial(E'/E)}{\partial \theta} = \frac{S' \sin \theta - P' \cos \theta \cos \phi - Q' \cos \theta \sin \phi}{S} = 0 \quad \Rightarrow \tag{61}$$

$$\tan \theta_e = \frac{P' \cos \phi_e + Q' \sin \phi_e}{S'} = \epsilon_1 \frac{\sqrt{(P')^2 + (Q')^2}}{S'} \Rightarrow \quad (62)$$

$$\cos \theta_e = \epsilon_2 \frac{S'}{\sqrt{(S')^2 + (P')^2 + (Q')^2}}, \quad \epsilon_2 = \pm 1. \quad (63)$$

The extreme value is then

$$\left( \frac{E'}{E} \right)_{\text{extreme}} = -\epsilon_2 \frac{\sqrt{(S')^2 + (P')^2 + (Q')^2}}{S}. \quad (64)$$

Since  $(\sin \theta_e \cos \phi_e, \sin \theta_e \sin \phi_e, \cos \theta_e) = \epsilon_2 (P', Q', S') / \sqrt{(P')^2 + (Q')^2 + (S')^2}$ , eq. (55) shows that the extreme values of  $E'/E$  are poles to the great circles of  $E' = 0$ . The latter can now be written in parametric form as

$$\cos \theta = -\cos \psi \sin \theta_e, \quad (65)$$

$$\tan \phi = \frac{\cos \theta_e \tan \phi_e + \tan \psi}{\cos \theta_e - \tan \phi_e \tan \psi} \quad (66)$$

Clearly  $E'/E$  has a dipole variation around each constant  $r$  sphere, changing sign when we go over to the antipodal point:  $(\theta, \phi) \rightarrow (\pi - \theta, \phi + \pi)$ . Writing

$$\left( R' - R \frac{E'}{E} \right) = \left( R' + R \frac{S' \cos \theta + \sin \theta (P' \cos \phi + Q' \sin \phi)}{S} \right) \quad (67)$$

we see that  $RE'/E$  is the correction to the radial separation  $R'$  of neighbouring constant  $r$  shells, due to their not being concentric. In particular  $RS'/S$  is the forward ( $\theta = 0$ ) displacement, and  $RP'/S$  &  $RQ'/S$  are the two sideways displacements ( $\theta = \pi/2, \phi = 0$ ) & ( $\theta = \pi/2, \phi = \pi/2$ ). The shortest 'radial' distance is where  $E'/E$  is maximum.

It will be shown in section 5.2 that, where  $R' > 0$ ,  $E'/E \leq M'/(3M)$  and  $E'/E \leq R'/R$  are required to avoid shell crossings, and also in eq (130) that  $R'/R > M'/3M$ . These inequalities, together with  $M' > 0$ , imply that the density given by (20), as a function of  $x = E'/E$ :

$$\rho = \frac{2M'}{R^2 R'} \frac{1 - 3Mx/M'}{1 - Rx/R'} \quad (68)$$

has a negative derivative by  $x$ :

$$\rho_{,x} = \frac{R/R' - 3M/M'}{(1 - Rx/R')^2} \cdot \frac{2M'}{R^2 R'} < 0, \quad (69)$$

and so the density is minimum where  $E'/E$  is maximum.

The density, eq. (20), can be decomposed into a spherical part and a dipole-like part, as noted by Szekeres [25] and de Souza [9] (see also p. 30 in Ref.[17]). Rewriting de Souza's result into our notation of eqs. (1) and (2), we obtain:

$$\rho = \rho_s + \Delta \rho, \quad (70)$$

where  $\rho_s$  is the spherical part:

$$\rho_s = \frac{2M'(A+C) - 6M(A'+C')}{R^2[R'(A+C) - R(A'+C')]} , \quad (71)$$

and  $\Delta\rho$  is the dipole-like part:

$$\Delta\rho = \frac{A'+C' - (A+C)E'/E}{R' - RE'/E} \cdot \frac{6MR' - 2M'R}{R^2[R'(A+C) - R(A'+C')]} . \quad (72)$$

The dipole-like part changes sign on the surface where  $E'/E = (A'+C')/(A+C)$ , but lacks the antisymmetry property:  $\Delta\rho(-E'/E) \neq -\Delta\rho(E'/E)$ . It can be verified (see Appendix A) that the  $\Delta\rho = 0$  hypersurface does intersect every ( $t = \text{const}$ ,  $r = \text{const}$ ) sphere along a circle, unless  $P' = Q' = S' = 0$  ( $= A' = C'$ ), in which case the dipole component of density is simply zero. The surface  $\Delta\rho = 0$  in a  $t = \text{const}$  space is comoving, i.e. its definition does not depend on  $t$ . Also, its intersection with any sphere of constant  $r$ ,  $E'/E = (A'+C')/(A+C) = \text{const}$ , is a circle parallel to the great circle  $E' = 0$ , as noted after eq. (58). It will coincide with the  $E' = 0$  circle in those points where  $A' + C' = 0$  (if they exist). The dipole-like component will be antisymmetric with respect to  $E'/E$  only at such values of  $r$ , where  $(A+C)R = 0 = (A'+C')R'$ , but such values may exist only at the center,  $R = 0$ , because  $A + C = 0$  contradicts eq. (3).

In the maximum ( $\epsilon_2 = -1$ ) and minimum ( $\epsilon_2 = 1$ ) directions,

$$E''_{\max/\min} = \frac{S(S''S' + P''P' + Q''Q') - [(S')^2 + (P')^2 + (Q')^2](2S' + \epsilon_2\sqrt{(S')^2 + (P')^2 + (Q')^2})}{S(S' - \epsilon_2\sqrt{(S')^2 + (P')^2 + (Q')^2})} , \quad (73)$$

while around the  $E' = 0$  circle

$$E'' = \frac{(S')^2 + (P')^2 + (Q')^2}{S} - \frac{S''(P'\cos\phi + Q'\sin\phi) - S'(P''\cos\phi + Q''\sin\phi)}{\sqrt{(P'\cos\phi + Q'\sin\phi)^2 + (S')^2} - (P'\cos\phi + Q'\sin\phi)} . \quad (74)$$

## 4 Regular Origins

When  $\epsilon = +1$ ,  $R = 0$  occurs at an origin of spherical coordinates, e.g.  $R(t, 0) = 0$ ,  $\forall t$ , where the 2-spheres have no size. Similarly,  $\dot{R}(t, 0) = 0 = \ddot{R}(t, 0)$ , etc  $\forall t$ . There will be a second origin, at  $r = r_O$  say, in any closed, regular,  $f < 0$  model. Thus, by (11) and (6) and their combinations with (4) & (5), for each constant  $\eta$

$$\lim_{r \rightarrow 0} \frac{M}{f} = 0 \quad , \quad \lim_{r \rightarrow 0} f = 0 \quad , \quad \lim_{r \rightarrow 0} \frac{f^2}{M} = 0 . \quad (75)$$

The type of time evolution at the origin must be the same as its neighbourhood, i.e., along a constant  $t$  slice away from the bang or crunch, by (12) and (7),

$$0 < \lim_{r \rightarrow 0} \frac{|f|^{3/2}(t - a)}{M} < \infty . \quad (76)$$

Clearly, we need  $M \rightarrow 0$ ,  $f \rightarrow 0$  and

$$0 < \lim_{r \rightarrow 0} \frac{|f|^{3/2}}{M} < \infty. \quad (77)$$

Using l'Hôpital's rule, this gives

$$\lim_{r \rightarrow 0} \frac{3Mf'}{2M'f} = 1. \quad (78)$$

The density and Kretschmann scalar must be well behaved. We don't consider a vacuum region of finite size at the origin, as that is just Minkowski space,  $M = 0$ , and we don't consider the obscure case of a single vacuum point at the origin. Because  $\rho$  &  $\bar{\rho}$  in (21) evolve differently, we also need

$$0 < \lim_{r \rightarrow 0} \frac{6M}{R^3} = \lim_{r \rightarrow 0} \frac{2M'}{R^2 R'} < \infty \quad \Rightarrow \quad \lim_{r \rightarrow 0} \frac{3R'M}{RM'} = 1 \quad (79)$$

and

$$0 < \lim_{r \rightarrow 0} \frac{2(M' - 3ME'/E)}{R^2(R' - RE'/E)} = \lim_{r \rightarrow 0} \frac{2M'}{R^2 R'} \frac{(1 - 3ME'/M'E)}{(1 - RE'/R'E)} < \infty, \quad (80)$$

but in fact the latter is ensured by the former, and the anisotropic effect of  $E$  vanishes at the origin. However, since  $E'/E$  is restricted by the conditions for no shell crossings, it would be odd if  $\lim_{r \rightarrow 0} ME'/M'E$  or  $\lim_{r \rightarrow 0} RE'/R'E$  were divergent. Since

$$\begin{aligned} R^2 \frac{R'}{M'} &= -\frac{M^2}{(-f)^3} \left(1 - \frac{3Mf'}{2M'f}\right) \sin \eta (\eta - \sin \eta)(1 - \cos \eta) \\ &+ \frac{M^2}{(-f)^3} \left(1 - \frac{Mf'}{M'f}\right) (1 - \cos \eta)^3 \\ &- \frac{M^2 a'}{(-f)^{3/2} M'} \sin \eta (1 - \cos \eta), \end{aligned} \quad (81)$$

eqs. (77) and (78) above make the first term zero and the second non-zero at an origin for all  $0 < \eta < 2\pi$ , so we only need

$$\lim_{r \rightarrow 0} \frac{Ma'}{M'} < \infty. \quad (82)$$

Lastly, the metric must be well behaved, so  $E$  should have no unusual behaviour, such as  $S = 0$ , that would compromise a valid mapping of  $(dp^2 + dq^2)/E^2$  to the unit sphere. Also, to ensure the rate of change of proper radius with respect to areal radius is that of an origin,  $g_{rr}/(R')^2$  should be finite

$$0 < \lim_{r \rightarrow 0} \frac{(R' - RE'/E)^2}{(1 + f)(R')^2} < \infty \quad (83)$$

$$\Rightarrow 0 < \lim_{r \rightarrow 0} \left(1 - \frac{3ME'}{M'E}\right)^2 < \infty \Rightarrow -\infty \leq \lim_{r \rightarrow 0} \left| \frac{ME'}{M'E} \right| < \infty \quad (84)$$

$$\text{and } \lim_{r \rightarrow 0} \left| \frac{ME'}{M'E} \right| \neq \frac{1}{3}, \quad (85)$$

where the last of (79) has been used. This should hold for all  $(p, q)$ , i.e. all  $(\theta, \phi)$ . Thus (57) gives

$$-\infty \leq \lim_{r \rightarrow 0} \left| \frac{MS'}{M'S} \right| < \infty, \quad -\infty \leq \lim_{r \rightarrow 0} \left| \frac{MP'}{M'S} \right| < \infty, \quad -\infty \leq \lim_{r \rightarrow 0} \left| \frac{MQ'}{M'S} \right| < \infty, \quad (86)$$

all three limits being different from 1/3.

All of the above suggests that, near an origin,

$$M \sim R^3, \quad f \sim R^2, \quad S \sim R^n, \quad P \sim R^n, \quad Q \sim R^n, \quad n \geq 0. \quad (87)$$

The condition  $E'/E \leq M'/3M$  that will be obtained in the next section implies that near an origin

$$n \leq 1 \quad (88)$$

## 5 Shell Crossings

### 5.1 Occurrence and Position of Shell Crossings in a Surface of Constant $t$ and $r$ .

A shell crossing, if it exists, is the locus of zeros of the function  $R' - RE'/E$ . Suppose that  $R' - RE'/E = 0$  holds for all  $r$  at some  $t = t_o$ . This leads to  $S' = P' = Q' = R' = 0$ . Since  $P$ ,  $Q$  and  $S$  depend only on  $r$ , this means they are constant throughout the spacetime. As seen from (1) and (20), the Szekeres metric reduces then to the LT metric, and so this case need not be considered.

Suppose that  $R' - RE'/E = 0$  holds for all  $t$  at some  $r = r_0$ . This is an algebraic equation in  $p$  and  $q$  whose coefficients depend on  $t$  and  $r$ . Taking the coefficients of different powers of  $p$  and  $q$  we find  $P' = Q' = S' = R' = 0$ , but this time these functions vanish only at  $r = r_0$ , while  $R'(t, r_0)$  will vanish for all  $t$ . This will either be a singularity (when  $M'(r_0) \neq 0$ ) or a neck (when  $M'(r_0) = 0$ ), familiar from the studies of the LT model, see Refs. [10] and [13]. Hence,  $R' - RE'/E \neq 0$  except at a shell crossing or at special locations.

Now  $R' > 0$  and  $R' - RE'/E < 0$  cannot hold for all  $p$  and  $q$ . This would lead to  $E' > ER'/R > 0$ , and we know that  $E'$  cannot be positive at all  $p$  and  $q$ . Hence, with  $R' > 0$ , there must be a region in which  $R' - RE'/E > 0$ . By a similar argument,  $R' < 0$  and  $R' - RE'/E > 0$  cannot hold for all  $p$  and  $q$ , so with  $R' < 0$ , there must be a region in which  $R' - RE'/E < 0$ .

Assuming  $R' > 0$ , can  $R' - RE'/E$  be positive for all  $p$  and  $q$ ? Writing

$$\begin{aligned} ER'/R - E' &= \frac{1}{2S} \left( \frac{S'}{S} + \frac{R'}{R} \right) \left[ (p - P)^2 + (q - Q)^2 \right] - \frac{1}{2} \epsilon S \left( \frac{S'}{S} - \frac{R'}{R} \right) \\ &\quad + \frac{1}{S} [(p - P)P' + (q - Q)Q'], \end{aligned} \quad (89)$$

the discriminants of this with respect to  $(p - P)$  and  $(q - Q)$  are

$$\Delta_p = \frac{P'^2}{S^2} - \frac{1}{S^2} \left( \frac{S'}{S} + \frac{R'}{R} \right) \left[ \left( \frac{S'}{S} + \frac{R'}{R} \right) (q - Q)^2 + (q - Q)Q' - \frac{1}{2} \epsilon \left( \frac{S'}{S} - \frac{R'}{R} \right) \right] \quad (90)$$

$$\Delta_q = 4 \frac{1}{S^2} \left( \frac{S'}{S} + \frac{R'}{R} \right)^2 \left[ \frac{P'^2 + Q'^2 + \epsilon S'^2}{S^2} - \epsilon \frac{R'^2}{R^2} \right]. \quad (91)$$

Thus  $ER'/R - E'$  will have the same sign for all  $p$  and  $q$  when  $\Delta_q < 0$  (because then also  $\Delta_p < 0$  for all  $q$ ). Hence,  $ER'/R - E'$  has the same sign for all  $p$  and  $q$  (i.e. there are no shell crossings) if and only if

$$\frac{R'^2}{R^2} > \epsilon \frac{P'^2 + Q'^2 + \epsilon S'^2}{S^2} := \Phi^2(r). \quad (92)$$

Note that when  $\epsilon = 0$ , this can fail only at those points where  $R' = 0$ .

If  $R'^2/R^2 = \Phi^2$ , then  $\Delta_q = 0$ , and so  $\Delta_p = 0$  at just one value of  $q = q_{SS}$ . At this value of  $q$ ,  $ER'/R - E' = 0$  at one value of  $p = p_{SS}$ . In this case, the shell crossing is a single point in the constant  $(t, r)$ -surface, i.e. a curve in a space of constant  $t$  and a 2-surface in spacetime.

If  $R'^2/R^2 < \Phi^2$ , then the locus of  $ER'/R - E' = 0$  is in general a circle (a straight line in the special case  $S'/S = -R'/R$ ) in the  $(p, q)$  plane. The straight line is just a projection onto the  $(p, q)$  plane of a circle on the sphere of constant  $t$  and  $r$ , and so is not really any special case.

When  $\Delta_q > 0$  ( $R'^2/R^2 < \Phi^2$ ), the two limiting values of  $q$  at which  $\Delta_p$  changes sign are

$$q_{1,2} = \frac{-Q' \pm \sqrt{P'^2 + Q'^2 + \epsilon (S'^2 - S^2 R'^2/R^2)}}{S'/S + R'/R}, \quad (93)$$

and then for every  $q$  such that  $q_1 < q < q_2$ , there are two values of  $p$  (only one if  $q = q_1$  or  $q = q_2$ ) such that  $ER'/R - E' = 0$ . These are

$$p_{1,2} = \frac{-P' \pm \sqrt{- \left[ \left( \frac{S'}{S} + \frac{R'}{R} \right) (q - Q) - Q' \right]^2 + P'^2 + Q'^2 + \epsilon (S'^2 - S^2 R'^2/R^2)}}{S'/S + R'/R}. \quad (94)$$

The values of  $p$  and  $q$  from (93) and (94) lie on the circle with the center at

$$(p_{SC}, q_{SC}) = \left( P - \frac{P'}{S'/S + R'/R}, Q - \frac{Q'}{S'/S + R'/R} \right), \quad (95)$$

and with the radius  $L_{SC}$  given by

$$L_{SC}^2 = \frac{P'^2 + Q'^2 + \epsilon (S'^2 - S^2 R'^2/R^2)}{(S'/S + R'/R)^2}. \quad (96)$$

This is in general a different circle than the one defined by  $E' = 0$ . As seen from (89), the shell crossing set intersects with the surface of constant  $t$  and  $r$  along the line  $E'/E = R'/R = \text{const}$ . As noted after eq. (58), this line is a circle that lies in a plane parallel to the  $E' = 0$  great circle. It follows immediately that the  $E' = 0$  and the SC circles cannot intersect unless they coincide.

## 5.2 Conditions for No Shell Crossings

Szekeres [25] obtained a number of regularity conditions for the  $\epsilon = +1$  metric, namely: (1) On any constant time slice,  $R(t = \text{const}, r)$  is monotonic in  $r$ , which allows a transformation

to make  $R = r$  and  $R' = 1$  on that slice. (2) At an origin,  $A, B_1, B_2 \& C$  should be  $C^1$ ,  $f = 0$ , and  $M \sim R^2$  but we are not sure why he required  $A' = 0 = B'_1 = B'_2 = C'$  there. (3) To keep the density non-singular,  $0 \leq ((S')^2 + (P')^2 + (Q')^2)/S^2 < \min((R'/R)^2, (M'/3M)^2)$ , which is a no shell crossing condition. We shall improve on the latter below.

For positive density, (20) shows that  $(M' - 3ME'/E) \& (R' - RE'/E)$  must have the same sign. We now consider the case where both are positive. Where  $(M' - 3ME'/E) \leq 0$  and  $(R' - RE'/E) < 0$  we reverse the inequalities in all the following.

In the case of both  $(M' - 3ME'/E) \& (R' - RE'/E)$  being zero, this can hold for a particular  $(p, q)$  value if  $M'/3M = R'/R$ , but the latter cannot hold for all time. This case can only hold for all  $(p, q)$  if  $M' = 0, E' = 0, R' = 0$ , which requires all of  $M', f', a', S', P', Q'$  to be zero at some  $r$  value.

We consider the inequality  $(M' - 3ME'/E) \geq 0$  and we argue that it must hold even for the extreme value of  $E'/E$ , (64), for which we obtain

$$\frac{M'}{3M} \geq \frac{E'}{E} \Big|_{max} = \frac{\sqrt{(S')^2 + (P')^2 + (Q')^2}}{S} \quad \forall r. \quad (97)$$

It is obvious that this is sufficient, and also that

$$M' \geq 0 \quad \forall r. \quad (98)$$

We will now consider  $(R' - RE'/E) > 0$  for all 3 types of evolution.

### 5.2.1 Hyperbolic evolution, $f > 0$

For hyperbolic models, we can write:

$$\frac{R'}{R} = \frac{M'}{M}(1 - \phi_4) + \frac{f'}{f} \left( \frac{3}{2}\phi_4 - 1 \right) - \frac{f^{3/2}a'}{M}\phi_5, \quad (99)$$

where

$$\phi_4 = \frac{\sinh \eta (\sinh \eta - \eta)}{(\cosh \eta - 1)^2}, \quad \phi_5 = \frac{\sinh \eta}{(\cosh \eta - 1)^2}. \quad (100)$$

At early times,

$$\eta \rightarrow 0, \quad (101)$$

$$R \rightarrow \frac{M}{f} \frac{\eta^2}{2} + O(\eta^4) \rightarrow 0, \quad (102)$$

$$\phi_5 \rightarrow \frac{4}{\eta^3} + O(\eta) \rightarrow +\infty, \quad (103)$$

$$\phi_4 \rightarrow \frac{2}{3} + O(\eta^2) \rightarrow \frac{2}{3}, \quad (104)$$

we find  $\phi_5$  dominates and

$$\frac{R'}{R} \rightarrow -\frac{f^{3/2}a'}{M}\phi_5, \quad (105)$$

so that  $(R' - RE'/E) > 0$  gives

$$a' < 0 \quad \forall r. \quad (106)$$

Similarly, at late times,

$$\eta \rightarrow \infty, \quad R \rightarrow \infty, \quad \phi_5 \rightarrow 0, \quad \phi_4 \rightarrow 1, \quad (107)$$

we find  $\phi_5$  vanishes and

$$\frac{R'}{R} \rightarrow \frac{1}{2} \frac{f'}{f}, \quad (108)$$

so that

$$\left( \frac{R'}{R} - \frac{E'}{E} \right) > 0 \quad \Rightarrow \quad \frac{f'}{2f} - \frac{E'}{E} > 0. \quad (109)$$

Following the above analysis of  $(M' - 3ME'/E) \geq 0$  we obtain

$$\frac{f'}{2f} > \frac{\sqrt{(S')^2 + (P')^2 + (Q')^2}}{S} \quad \forall r, \quad (110)$$

which obviously implies

$$f' > 0 \quad \forall r. \quad (111)$$

Again, since we already have  $M' \geq 0$ , it is clear that this is sufficient, and that

$$R' > 0. \quad (112)$$

### 5.2.2 Parabolic evolution, $f = 0$

The easiest way to obtain the conditions for this case,  $f = 0, f' \neq 0$ , is to put  $\tilde{\eta} = \eta/\sqrt{f} > 0$  in the hyperbolic case, and take the limit  $f \rightarrow 0, \eta \rightarrow 0$ . All terms involving  $f'/f$  cancel and we retain exactly the same conditions, viz (106) & (111) (and of course (97)). Naturally, (110) ceases to impose any limit.

### 5.2.3 Elliptic evolution, $f < 0$

For elliptic models, we can write:

$$\frac{R'}{R} = \frac{M'}{M}(1 - \phi_1) + \frac{f'}{f} \left( \frac{3}{2} \phi_1 - 1 \right) - \frac{(-f)^{3/2} a'}{M} \phi_2, \quad (113)$$

where

$$\phi_1 = \frac{\sin \eta (\eta - \sin \eta)}{(1 - \cos \eta)^2}, \quad \phi_2 = \frac{\sin \eta}{(1 - \cos \eta)^2}. \quad (114)$$

At early times,

$$\eta \rightarrow 0, \quad (115)$$

$$R \rightarrow \frac{M}{(-f)} \frac{\eta^2}{2} + O(\eta^4) \rightarrow 0, \quad (116)$$

$$\phi_2 \rightarrow \frac{4}{\eta^3} + O(\eta) \rightarrow +\infty, \quad (117)$$

$$\phi_1 \rightarrow \frac{2}{3} + O(\eta^2) \rightarrow \frac{2}{3}, \quad (118)$$

we find  $\phi_2$  dominates and

$$\frac{R'}{R} \rightarrow -\frac{f^{3/2}a'}{M}\phi_2, \quad (119)$$

so that  $R(R'/R - E'/E) > 0$  gives

$$a' < 0 \quad \forall r. \quad (120)$$

Similarly, at late times,

$$\eta \rightarrow 2\pi, \quad (121)$$

$$R \rightarrow \frac{M}{(-f)} \frac{(2\pi - \eta)^2}{2} + O((2\pi - \eta)^4) \rightarrow 0, \quad (122)$$

$$\phi_2 \rightarrow -4/(2\pi - \eta)^3 + O((2\pi - \eta)) \rightarrow -\infty, \quad (123)$$

$$\phi_1 \rightarrow -8\pi/(2\pi - \eta)^3 + 2/3 + O((2\pi - \eta)) \rightarrow -\infty, \quad (124)$$

we find

$$\frac{R'}{R} \rightarrow \frac{M'}{M} \left( \frac{8\pi}{(2\pi - \eta)^3} \right) - \frac{f'}{f} \left( \frac{12\pi}{(2\pi - \eta)^3} \right) + \frac{(-f)^{3/2}a'}{M} \left( \frac{4}{(2\pi - \eta)^3} \right), \quad (125)$$

so that  $R^{3/2}(R'/R - E'/E) > 0$  now gives

$$\frac{2\pi M}{(-f)^{3/2}} \left( \frac{M'}{M} - \frac{3f'}{2f} \right) + a' > 0 \quad \forall r, \quad (126)$$

which is the condition that the crunch time must increase with  $r$ . Since we already have  $M' \geq 0$ , it may be easily verified that these conditions are sufficient, to keep

$$R' > 0 \quad (127)$$

for all  $\eta$ .

We now show the above also ensure  $R(R'/R - E'/E) > 0$  always. Defining the crunch time  $b(r)$  with

$$b = a + \frac{2\pi M}{(-f)^{3/2}} \quad (128)$$

we can re-write (113) as

$$\frac{R'}{R} = \frac{M'}{3M} + \frac{b'}{(b-a)} \left( \frac{2}{3} - \phi_1 \right) + \frac{(-a')}{(b-a)} \left( \frac{2}{3} - \phi_1 + 2\pi\phi_2 \right). \quad (129)$$

The derivative of  $(2/3 - \phi_1)$  is  $(2\eta - 3\sin\eta + \eta\cos\eta)/(1 - \cos\eta)^2$ , and the third derivative of the numerator of the latter is  $\eta\sin\eta$ . It follows that  $(2/3 - \phi_1) \geq 0$  and declines monotonically from  $+\infty$  to 0 as  $\eta$  goes from  $2\pi$  to 0. Since  $(2/3 - \phi_1 + 2\pi\phi_2)$  is the mirror image in  $\eta = \pi$  of  $(2/3 - \phi_1)$ , we have that

$$\frac{R'}{R} > \frac{M'}{3M}, \quad (130)$$

so that (97) guarantees that for each given  $r$ , the maximum of  $E'/E$  as  $(p, q)$  are varied is no more than the minimum of  $R'/R$  as  $\eta$  varies.

Note that although (126) implies

$$\frac{f'}{2f} < \frac{M'}{3M}, \quad (131)$$

a condition such as (110) is not needed in this case. As an indication of what the approximate magnitude of  $R'/R|_{\min}$ , at the moment of maximum expansion along any given worldline,

$$\frac{R'}{R} = \frac{M'}{M} - \frac{f'}{f}, \quad (132)$$

so it would be possible to have  $E'/E|_{\max}$  close to  $R'/R|_{\min}$  around the time of maximum expansion.

## 6 Regular Maxima & Minima

Certain topologies necessarily have extrema in  $R$ . For example, closed spatial sections have a maximum areal radius, and wormholes have a minimum areal radius, i.e.  $R'(t, r_m) = 0, \forall t$ .

Suppose  $(\epsilon + f) = 0$  at some  $r = r_m$ . By (41) we must have

$$f'(r_m) = 0 \quad (133)$$

(unless  $f'$  is discontinuous there, which we won't consider). We need  $(R' - RE'/E) = 0$  to keep  $g_{rr}$  finite, and hence  $(M' - 3ME'/E) = 0$  to keep  $\rho$  finite, both holding  $\forall (t, p, q)$  at that  $r_m$ . More specifically, along any given spatial slice away from the bang or crunch, we want

$$\frac{(R' - RE'/E)}{\sqrt{\epsilon + f}} \rightarrow L, \quad 0 < L < \infty, \quad (134)$$

$$\frac{(M' - 3ME'/E)}{(R' - RE'/E)} \rightarrow N, \quad 0 \leq N < \infty. \quad (135)$$

As noted above, we require

$$M' = f' = a' = S' = P' = Q' = 0 \quad (136)$$

to ensure

$$R' = 0. \quad (137)$$

The limits (134) and (135) must hold good for all  $t$  and for all  $(p, q)$ , so using (13), (99) & (113) with  $R > 0, M > 0, S > 0$  shows that

$$\frac{M'}{\sqrt{\epsilon + f}}, \quad \frac{f'}{\sqrt{\epsilon + f}}, \quad \frac{a'}{\sqrt{\epsilon + f}}, \quad \frac{R'}{\sqrt{\epsilon + f}}, \quad (138)$$

$$\frac{S'}{\sqrt{\epsilon + f}}, \quad \frac{P'}{\sqrt{\epsilon + f}}, \quad \frac{Q'}{\sqrt{\epsilon + f}}, \quad \frac{E'}{\sqrt{\epsilon + f}} \quad (139)$$

must all have finite limits, that do not have to be zero. Using l'Hôpital's rule, each of the above limits can be expressed in the form

$$L_{M'} = \lim_{f \rightarrow -1} \frac{M'}{\sqrt{\epsilon + f}} = \frac{2M''\sqrt{\epsilon + f}}{f'} = \frac{2M''}{L_{f'}}. \quad (140)$$

Thus, for  $f = -1$ , the above conditions for no shell crossings in elliptic regions should be re-expressed in terms of these limits.

It is worth pointing out that  $E' = 0$  at  $f = -1$  does not imply the shells near an extremum in  $R$  are concentric. It is the above limits that determine whether there is non-concentricity at  $f = -\epsilon$ .

Conversely, imposing  $R' = 0$  forces all of (136), if we are to avoid shell crossings. To obtain  $f = -\epsilon$ , we must impose one further requirement for a regular extremum — that no surface layers should occur at  $r = r_m$ . Using the results for the normal  $n_\mu$  and the extrinsic curvature  $K_{ij}$  shown in the next section, and choosing the junction surface to be at constant coordinate radius,  $r = Z = r_m$ , the non-zero components are:

$$n_r = -\frac{(R' - RE'/E)}{\sqrt{\epsilon + f}}, \quad (141)$$

$$K_{pp} = \frac{-R(\epsilon + f)^{1/2}}{E^2}, \quad (142)$$

$$K_{qq} = \frac{-R(\epsilon + f)^{1/2}}{E^2}. \quad (143)$$

Now at an extremum in  $R$ , the factor  $(R' - RE'/E)$  goes from positive to negative (because where  $(R' - RE'/E) < 0$ , the no-shell-crossing conditions require  $R' < 0$ ), which means that  $n_\mu$  flips direction. For a boundary with no surface layer we must have  $n_\mu$  pointing the same way on both sides, towards increasing  $r$  say, and zero jump in the extrinsic curvature. So, if we cut the model at the maximum or minimum  $r_m$ , and match the two halves back together, we need

$$K_{ij}^+(-n_\mu) = K_{ij}^-(+n_\mu) \quad \Rightarrow \quad K_{ij}^+ = -K_{ij}^-, \quad (144)$$

which is only possible if

$$f = -\epsilon. \quad (145)$$

If however,  $r_m$  is only a shoulder — i.e.  $R'(r_m) = 0$ , but  $R'$  has the same sign on either side, then the normal direction does not change sign, so there is no surface layer even if  $f \neq -\epsilon$ . However  $g_{rr} = L^2$  goes to zero, so it is likely that a change of coordinates could make  $|R'| > 0$ .

## 6.1 Summary: Conditions for No Shell Crossings or Surface Layers

The conditions found here are exactly those on  $M$ ,  $f$  &  $a$  for LT models (see [13] which generalises those of [1] for  $a = 0$  LT models), with extra conditions involving  $S$ ,  $P$ ,  $Q$  also.

$\epsilon$	$R'$	$f$	$M', f', a'$	$S', P', Q'$
+1	$> 0$	all	$M' \geq 0$	$\frac{\sqrt{(S')^2 + (P')^2 + (Q')^2}}{S} \leq \frac{M'}{3M}$
+1	$> 0$	$\geq 0$	$f' \geq 0$ $a' \leq 0$ but not all 3 equalities at once	$\frac{\sqrt{(S')^2 + (P')^2 + (Q')^2}}{S} \leq \frac{f'}{2f}$ (no condition where $f = 0$ )
+1	$> 0$	$< 0$	$\frac{2\pi M}{(-f)^{3/2}} \left( \frac{M'}{M} - \frac{3f'}{2f} \right) + a' \geq 0$ $a' \leq 0$ but not all 3 equalities at once	
+1	$= 0$ $R'' > 0$ neck	$-1$	$M' = 0, f' = 0, a' = 0$ ( $f = -1$ for no surface layer) $\frac{2\pi M}{(-f)^{3/2}} \left( \frac{M''}{M} - \frac{3f''}{2f} \right) + a'' \geq 0$ $a'' \leq 0$	$S' = 0, P' = 0, Q' = 0$ $\frac{\sqrt{(S'')^2 + (P'')^2 + (Q'')^2}}{S} \leq \frac{M''}{3M}$
+1	$= 0$ $R'' < 0$ belly	$-1$	$M' = 0, f' = 0, a' = 0$ ( $f = -1$ for no surface layer) $\frac{2\pi M}{(-f)^{3/2}} \left( \frac{M''}{M} - \frac{3f''}{2f} \right) + a'' \leq 0$ $a'' \geq 0$	$S' = 0, P' = 0, Q' = 0$ $-\frac{\sqrt{(S'')^2 + (P'')^2 + (Q'')^2}}{S} \geq \frac{M''}{3M}$
+1	$< 0$	all	$M' \leq 0$	$-\frac{\sqrt{(S')^2 + (P')^2 + (Q')^2}}{S} \geq \frac{M'}{3M}$
+1	$< 0$	$\geq 0$	$f' \leq 0$ $a' \geq 0$ but not all 3 equalities at once	$-\frac{\sqrt{(S')^2 + (P')^2 + (Q')^2}}{S} \geq \frac{f'}{2f}$ (no condition where $f = 0$ )
+1	$< 0$	$< 0$	$\frac{2\pi M}{(-f)^{3/2}} \left( \frac{M'}{M} - \frac{3f'}{2f} \right) + a' \leq 0$ $a' \geq 0$ but not all 3 equalities at once	

## 7 Impossibility of a Handle Topology

Since the function  $E$  has the effect of making the distance between adjacent constant  $r$  shells depend on angle, this allows us to create a wormhole that is bent, so that the two asymptotic world sheets on either side can be thought of as intersecting in the embedding.

This leads to the question of whether those two world sheets can be smoothly joined across a junction surface. In fact the possibility of matching the two world sheets together can be considered independently of whether there is a natural embedding that would allow them to intersect at the appropriate angles.

Thus we investigate whether it is possible to create a Szekeres model with a handle topology in the following way. Take a wormhole topology — an  $\epsilon = +1$  model with  $r = 0, f(0) = -1$  at the wormhole &  $f < 0$  nearby — and let it be mirror symmetric about  $r = 0$ . Choose a comoving open surface  $\Sigma$  on one side of the wormhole, and its mirror image on the other side, and match the two sheets together along  $\Sigma$ , as shown schematically in Fig. 3. Because the 2 sheets are mirror images, this is equivalent to matching  $\Sigma$  to its own mirror image.

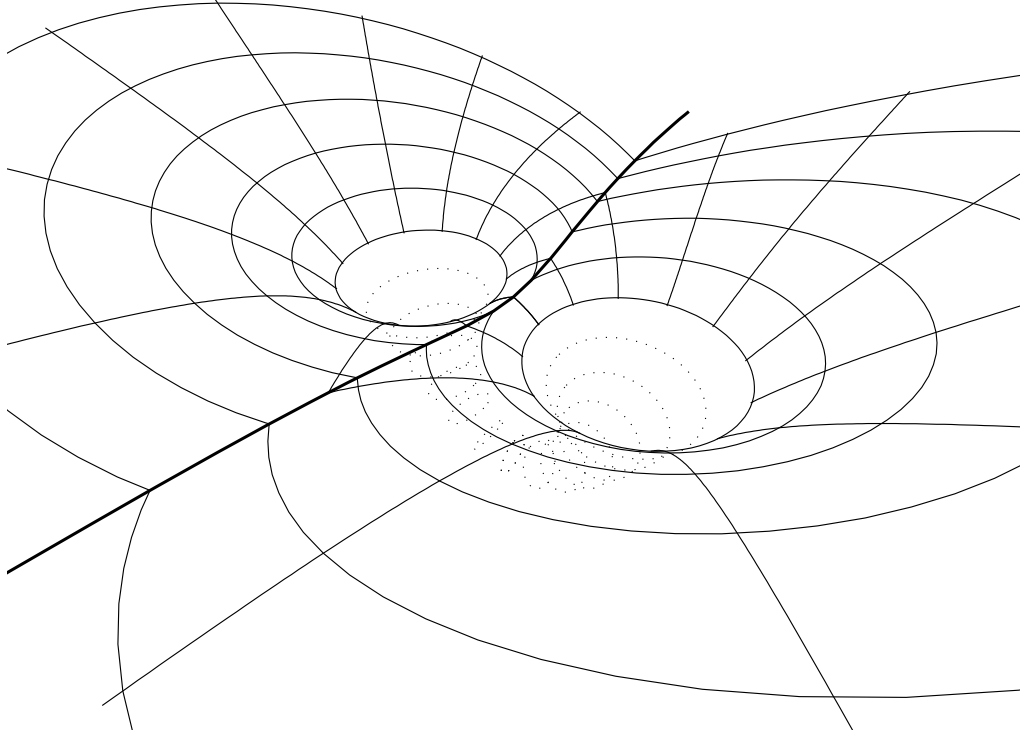


Figure 3: Conceptual illustration of joining a Szekeres wormhole model to itself across a boundary surface  $\Sigma$ , shown as a heavy line. The boundary may be close to the wormhole, as shown, or out in the asymptotic regions. There is no significance to the change from solid to dotted circles, other than picture clarity. The handle topology is shown as an embedding of a constant time section, with one angular coordinate suppressed, although a valid matching across  $\Sigma$  does not require the result to have a natural embedding. However, it is shown that the matching fails because it is not preserved by the model evolution.

To implement this we choose a comoving surface:

$$r_\Sigma = Z(p, q) \quad (146)$$

and surface coordinates:

$$\xi^i = (t, p, q). \quad (147)$$

The two fundamental forms and the normal are calculated in appendix B.

Obviously 1st fundamental forms match by construction, and normal vectors are equal and opposite:

$$n_\mu^+ = -n_\mu^- . \quad (148)$$

In fact the 2 surfaces  $\Sigma^+$  &  $\Sigma^-$  are identical except for the sign of  $n_\mu$ . Thus  $K_{ij}^- = -K_{ij}^+$ , so the only way to match the 2nd fundamental forms,  $K_{ij}^+ = K_{ij}^-$ , is to make them zero:

$$K_{ij}^\pm = 0. \quad (149)$$

The  $K_{pt} = -K_{pt}$  &  $K_{qt} = -K_{qt}$  equations give

$$R' = 0 \quad \Rightarrow \quad r_\Sigma \text{ is at a shell crossing unless } Z = \text{ const} \quad (150)$$

$$\text{or } \dot{R} = 0 \quad \Rightarrow \quad \text{Static: Not possible} \quad (151)$$

$$\text{or } Z_p = 0, \quad Z_q = 0 \quad \Rightarrow \quad r_\Sigma = Z = \text{constant.} \quad (152)$$

If the matching surface is at constant  $r$ , then only a closed torus topology is possible. So the answer is: no, a handle topology is not possible.

Suppose  $\dot{R} = 0$  possible, then it should be possible to solve

$$K_{pp} = 0 , \quad K_{pq} = 0 , \quad K_{qq} = 0 \quad (153)$$

for  $Z(p, q)$ , by specifying suitable functions  $E(r, p, q)$  &  $R(r)$  on an initial time slice. In other words, you can probably match on a constant time slice, but the matching is not preserved by the model evolution.

## 8 Szekeres Wormholes?

It has been shown in [10] that LT models can describe the Schwarzschild-Kruskal-Szekeres manifold, as well as models that have the same topology but non-zero density. It has also been shown that the matter flows from past to future singularity, with possibly some matter escaping to  $\mathcal{J}^+$  or some being captured from  $\mathcal{J}^-$ . The effect of the introduction of matter on the causal structure is to split the Kruskal event horizons and reduce communication through the wormhole. The locus  $R = 2M$  is an apparent horizon, but not an event horizon, and light rays fall irrevocably through the AH towards the singularity wherever  $M' > 0$ . Only if the density is (locally) zero is  $R = 2M$  (locally) null. Only if the density is everywhere zero is  $R = 2M$  the event horizon. (See also [1] for a study of light rays and AHs in a collapsing LT model with  $a = 0$ .)

Since LT models are a subset of Szekeres models, it is of interest to look at the properties of the Szekeres generalisation, and determine how the loss of spherical symmetry in the Szekeres model affects the LT result.

In particular, given the anisotropy of the metric and the fact that the proper separation of constant  $r$  shells varies with  $p$  &  $q$ , is it possible for null or timelike paths to pass through a neck or wormhole, by choosing a path along which distances have been made shorter by the particular form of  $E$ ? In other words, can one construct a Szekeres wormhole that is traversible?

For a wormhole, we require an elliptic region, in order to create a “neck” – a regular minimum in  $R(t = \text{const}, r)$ ,

$$-1 \leq f < 0 , \quad \epsilon = +1 , \quad (154)$$

but the asymptotic regions may be described by elliptic, parabolic, or hyperbolic regions.

### 8.1 The Fastest Way Out

The general null condition gives

$$0 = k^\alpha k^\beta g_{\alpha\beta} = (-1) (k^t)^2 + \frac{\left(R' - R \frac{E'}{E}\right)^2}{\epsilon + f} (k^r)^2 + \frac{R^2}{E^2} ((k^p)^2 + (k^q)^2) \quad (155)$$

$$\Rightarrow \frac{\left(R' - R \frac{E'}{E}\right)^2}{\epsilon + f} \left(\frac{dr}{dt}\right)^2 = 1 - \frac{R^2}{E^2} \left(\left(\frac{dp}{dt}\right)^2 + \left(\frac{dq}{dt}\right)^2\right) . \quad (156)$$

It is obvious that at each event  $dr/dt$  is maximised by choosing  $k^p = 0 = k^q$ . Since  $R$  is independent of  $(p, q)$ , this also gives the direction of maximum  $dR/dt|_{null}$  at any event. We will call this “radial” motion, and radial null paths “rays”. Thus, the DE

$$t'_n = \frac{dt}{dr} \Big|_n = \frac{j}{\sqrt{1+f}} \left( R' - \frac{RE'}{E} \right) , \quad j = \pm 1 \quad (157)$$

in principle solves to give

$$t = t_n(r) \quad (158)$$

along the “ray”. We don’t expect this to be geodesic, but we regard it as the limit of a sequence of accelerating timelike paths, and thus the boundary to possible motion through a wormhole. The acceleration of this path may be calculated from  $a^\alpha = k^\beta \nabla_\beta k^\alpha$ , as given in appendix C.

## 8.2 Apparent Horizons

The areal radius along a ‘ray’ is

$$R_n = R(t_n(r), r), \quad (159)$$

$$(R_n)' = \dot{R} t'_n + R' \quad (160)$$

$$= j \frac{\dot{R}}{\sqrt{1+f}} \left( R' - \frac{RE'}{E} \right) + R' \quad (161)$$

$$= \ell j \frac{\sqrt{\frac{2M}{R} + f}}{\sqrt{1+f}} \left( R' - \frac{RE'}{E} \right) + R' , \quad \ell = \pm 1. \quad (162)$$

These rays are momentarily stationary when

$$(R_n)' = 0. \quad (163)$$

Now light rays initially along constant  $p$  and  $q$  will not remain so, owing to the anisotropy of the model. However, since these “radial” directions are at each point the fastest possible escape route, we define this locus to be the apparent horizon (AH).

(Szekeres [25] defined a trapped surface as the locus where null geodesics that are (momentarily) ‘radial’ have zero divergence,  $k^\mu_{;\mu} = 0$ , where  $k^\mu_{;\nu} k_\nu = 0$ ,  $k_\mu k^\mu = 0$ ,  $k^p = 0 = k^q$ . He obtained

$$k^\mu_{;\mu} = \frac{2}{R} \left( R' - \frac{RE'}{E} \right) \left( \frac{\dot{R}}{\sqrt{1+f}} + j \right). \quad (164)$$

Given the anisotropy of the model, one doesn’t expect this to be the same locus as our AH.)

Assuming a normal spacetime point will have non-zero metric components, and taking  $R$  increasing with  $r$  on constant  $t$  slices,

$$R' > 0 \quad \text{and} \quad \left( R' - \frac{RE'}{E} \right) > 0, \quad (165)$$

we require

$$\ell j = -1, \quad (166)$$

i.e.

$$\begin{aligned} \text{Either (future AH: AH}^+ \text{)} \quad j &= +1 & \text{(outgoing rays)} \\ \ell &= -1 & \text{(in a collapsing phase)} \end{aligned} \quad (167)$$

$$\begin{aligned} \text{Or (past AH: AH}^- \text{)} \quad j &= -1 & \text{(incoming rays)} \\ \ell &= +1 & \text{(in an expanding phase).} \end{aligned} \quad (168)$$

Note that we want 'outgoing' to mean moving away from the neck at  $r = 0$ . A ray passing through the neck would change from incoming to outgoing at  $r = 0$ , and, since  $R'$  flips sign there,  $j$  would also have to flip there.

### 8.2.1 The Apparent Horizon and its Location with Respect to $E' = 0$ .

Define

$$D := \sqrt{1+f} - \sqrt{\frac{2M}{R} + f}. \quad (169)$$

Then

$$(D > 0) \iff (R > 2M). \quad (170)$$

Since  $M/R$  and  $(2M/R + f)$  are positive, we see that  $D \geq 1$  leads to a contradiction, and so

$$D < 1. \quad (171)$$

However,  $|D|$  can be greater than 1 because  $D < -1$  is not prohibited. We have

$$(D < -1) \implies \left( R < \frac{M}{1 + \sqrt{1+f}} \right). \quad (172)$$

This will always occur when  $R$  is close to the Big Bang/Big Crunch.

Using  $D$ , the equation of the AH is

$$RE' + DR'E = 0, \quad (173)$$

and in terms of  $p$  and  $q$  this equation is

$$\left( \frac{S'}{S} - D \frac{R'}{R} \right) \left[ (p - P)^2 + (q - Q)^2 \right] + 2[(p - P)P' + (q - Q)Q'] - S^2 \left( \frac{S'}{S} + D \frac{R'}{R} \right) = 0. \quad (174)$$

The discriminant of this with respect to  $p$  is

$$\Delta_p = 4P'^2 - 4 \left( \frac{S'}{S} - D \frac{R'}{R} \right) \left[ \left( \frac{S'}{S} - D \frac{R'}{R} \right) (q - Q)^2 + 2(q - Q)Q' - S^2 \left( \frac{S'}{S} + D \frac{R'}{R} \right) \right]. \quad (175)$$

The discriminant of this with respect to  $q$  is

$$\Delta_q = 64 \left( \frac{S'}{S} - D \frac{R'}{R} \right)^2 \left[ P'^2 + Q'^2 + S^2 \left( \frac{S'^2}{S^2} - D^2 \frac{R'^2}{R^2} \right) \right]. \quad (176)$$

Now, if  $\Delta_q < 0$  everywhere, then  $\Delta_p < 0$  for all  $q$ , in which case there is no  $p$  obeying (174), i.e. the apparent horizon does not intersect this particular surface of constant  $(t, r)$ .

If  $\Delta_q = 0$ , then  $\Delta_p < 0$  for all  $q$  except one value  $q = q_0$ , at which  $\Delta_p = 0$ . At this value of  $p = p_0$ , (174) has a solution, and so the intersection of the apparent horizon with this one constant  $(t, r)$  surface is a single point. Note that the situation when the apparent horizon touches the whole 3-dimensional  $t = \text{const}$  hypersurface at a certain value of  $t$  is exceptional, this requires, from (174), that  $P' = Q' = S' = R' = 0$  at this value of  $t$ . The first three functions being zero mean just spherical symmetry, but the fourth one defines a special location, as mentioned at the beginning of sec. 5.1. These equations hold in the Datt-Ruban [8, 21, 22] solution.

If  $\Delta_q > 0$ , then  $\Delta_p > 0$  for every  $q$  such that  $q_1 < q < q_2$ , where

$$q_{1,2} = \frac{-Q' \pm \sqrt{P'^2 + Q'^2 + S^2 \left( \frac{S'^2}{S^2} - D^2 \frac{R'^2}{R^2} \right)}}{S'/S - DR'/R} \quad (177)$$

and then a solution of (174) exists given by

$$p_{1,2} = \frac{-P' \pm \sqrt{- \left[ \left( \frac{S'}{S} - D \frac{R'}{R} \right) (q - Q) + Q' \right]^2 + P'^2 + Q'^2 + S^2 \left( \frac{S'^2}{S^2} - D^2 \frac{R'^2}{R^2} \right)}}{S'/S - DR'/R}. \quad (178)$$

Except for the special case when  $S'/S = DR'/R$ , these values lie on a circle in the  $(p, q)$  plane, with the center at

$$(p_{AH}, q_{AH}) = \left( P - \frac{P'}{S'/S - DR'/R}, Q - \frac{Q'}{S'/S - DR'/R} \right), \quad (179)$$

and with the radius  $L_{AH}$  given by

$$L_{AH}^2 = \frac{P'^2 + Q'^2 + S^2 \left( \frac{S'^2}{S^2} - D^2 \frac{R'^2}{R^2} \right)}{(S'/S - DR'/R)^2}. \quad (180)$$

The special case  $S'/S = DR'/R$  (when the locus of AH in the  $(p, q)$  plane is a straight line) is again an artefact of the Riemann projection because this straight line is an image of a circle on the sphere.

In summary, the intersection of AH with the  $(p, q)$ -plane is

- nonexistent when  $R'^2/R^2 > \Phi^2/D^2$  (this is the same  $\Phi$  as for the shell crossing);
- a single point when  $R'^2/R^2 = \Phi^2/D^2$ ;
- a circle or a straight line when  $R'^2/R^2 < \Phi^2/D^2$ .

The condition  $R'^2/R^2 < \Phi^2/D^2$  is consistent with the condition for no shell crossings, eq. (92), when  $|D| < 1$ . We already know that necessarily  $D < 1$ , but  $D < -1$  is not excluded.

With  $|D| < 1$ , when the intersection of AH with  $(t = \text{const}, r = \text{const})$  is a single point, a shell crossing is automatically excluded.

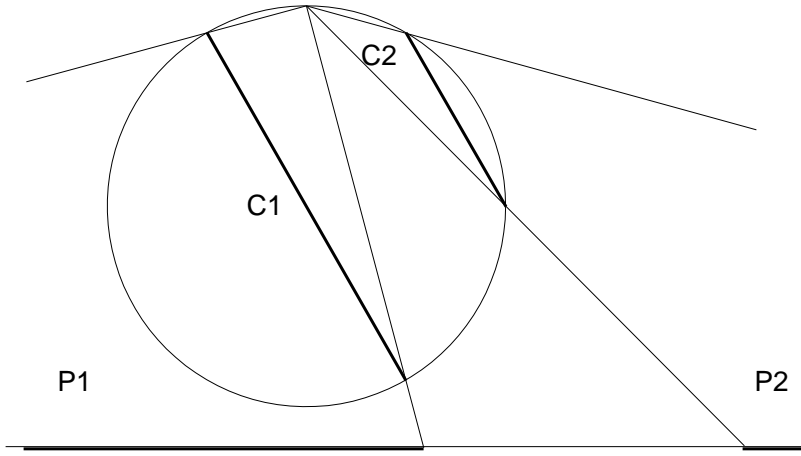


Figure 4: The circles  $C_1$  and  $C_2$  on a sphere (seen here edge on) will project onto the plane (seen here as the horizontal line) as the circles  $P_1$  and  $P_2$  that are outside each other. Only parts of  $P_1$  and  $P_2$  are shown here. Circle  $C_1$  is the  $E' = 0$  set, circle  $C_2$  is the apparent horizon circle.

Note that from (173) and from the assumptions  $R > 0$ ,  $E > 0$  and  $R' > 0$  we have

$$\begin{aligned} (D > 0) &\implies (E' < 0) \\ (D < 0) &\implies (E' > 0). \end{aligned} \tag{181}$$

But  $D > 0$  and  $D < 0$  define regions independent of  $p$  and  $q$ . Hence, on that surface, on which  $D > 0$ ,  $E' < 0$  on the whole of AH. Where  $D < 0$ ,  $E' > 0$  on the whole of AH. This implies that the  $E' = 0$  circle and the AH cannot intersect unless they coincide. Indeed, these circles lie in parallel planes, by the same argument that was used at the end of sec. 5.1: the line on the  $(t, r) = \text{const}$  surface defined by (173) has the property  $E'/E = -DR'/R = \text{const}$ , and so it must be a circle in a plane parallel to the  $E' = 0$  great circle. It follows that of the three circles ( $E' = 0$ , SC and AH), no two can intersect unless they coincide.

When the  $E' = 0$  and AH circles are disjoint, they may either be one inside the other or each one outside the other. However, when projected back onto the sphere, these two situations turn out to be topologically equivalent: depending on the position of the point of projection, the same two circles may project onto the plane either as one circle inside the other or as two separate circles, see Figs. 4 and 5.

### 8.2.2 Location of the AH Compared with $R = 2M$

Along  $R = 2M$

$$(R_n)' = R'(1 + \ell j) - \frac{RE'}{E}, \tag{182}$$

so  $R = 2M$  is not the AH except where  $E' = 0$ .

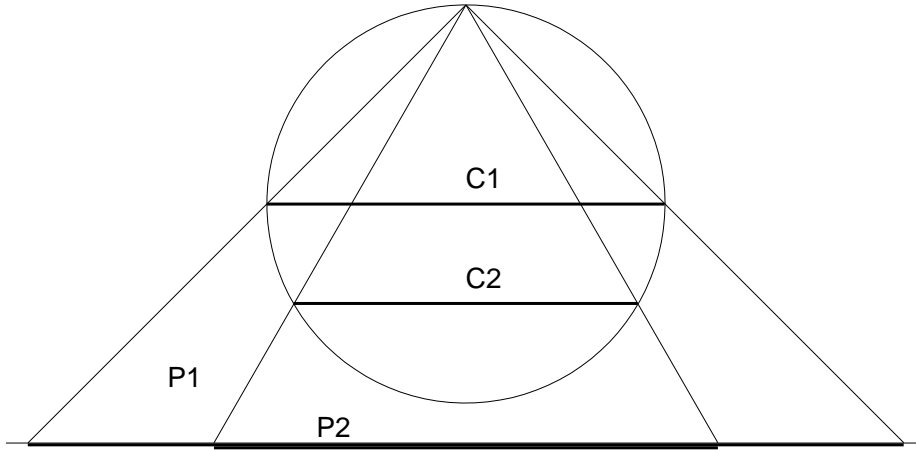


Figure 5: The same circles as in Fig. 4 projected onto a plane from a different pole will project as one inside the other. The transition from the situation of Fig. 4 to that of Fig. 5 is continuous and occurs when the sphere is rotated, but the pole and the plane are not moved. Then one of the circles (C1 when a clockwise rotation is applied to Fig. 4) will pass through the pole at one value  $\varphi = \varphi_0$  of the rotation angle. Its image on the plane is acquiring a larger and larger radius with increasing  $\varphi$ , until it becomes a straight line when  $\varphi = \varphi_0$ . When  $\varphi$  increases further, the straight line bends in the opposite direction so that it surrounds the second circle P2.

Eq (162) with (163) and  $\ell j = -1$  can be written

$$\Rightarrow R_{AH} = \frac{2M(1 - RE'/R'E)^2}{1 + f[1 - (1 - RE'/R'E)^2]} \quad (183)$$

$$= \frac{2M(1 - V)^2}{1 + f(2V - V^2)} , \quad V = RE'/R'E. \quad (184)$$

The effect of  $E(r, p, q)$  is to create a dipole in the geometry and density around each  $(t, r)$  shell, with  $E' = 0$  on an “equator”, and extreme values

$$\left. \frac{E'}{E} \right|_{\text{extreme}} = \pm \frac{\sqrt{(S')^2 + (P')^2 + (Q')^2}}{S} \quad (185)$$

at the poles.

It is clear then that “radial” displacements between two nearby surfaces of constant  $r$  are shortest where  $E'/E$  is maximum, and light rays move outwards fastest ( $\max dr/dt, \min dt/dr$ , i.e. most rapid transfer between constant  $r$  shells at the same  $(p, q)$  value). It has also been shown that the density is minimum here. The longest “radial” displacements, slowest light ray motion and maximum density occurs at the opposite pole.

We will call the direction where  $E'/E$  is maximum, the ‘fast’ pole, and where  $E'/E$  is minimum, the ‘slow’ pole.

Now the conditions for no shell crossings require

$$\left. \frac{E'}{E} \right|_{\text{extreme}} < \frac{M'}{3M} \quad (186)$$

and for an elliptic region we have

$$\frac{M'}{3M} < \frac{R'}{R}, \quad (187)$$

so

$$V^2 < 1, \quad (1 - V)^2 > 0, \quad -3 < (2V - V^2) < 1. \quad (188)$$

In those places on the AH, where  $V = 0 = E'$ , we see that the surface  $R = 2M$  intersects the AH at all times, but the AH is a kind of oval with half inside  $R = 2M$  and half outside.

For  $f = -1$

$$\frac{R_{AH}}{2M} = 1 \quad (189)$$

regardless of  $V$ . So it is clear that  $AH^+$  &  $AH^-$  cross in a 2-sphere at the neck of the wormhole ( $f = -1$ ) at the moment of maximum expansion ( $R = 2M$ ), as in LT. Note also that at the bang, wherever  $a' \neq 0$ ,  $R \rightarrow 0$  and  $R' \rightarrow \infty$  imply  $V \rightarrow 0$ , and the anisotropy becomes negligible. Similarly for the crunch.

But in general, for all  $0 \geq f > -1$

$$\frac{4}{1 + 3|f|} \geq \frac{R_{AH}}{2M} \geq 0 \quad (190)$$

and  $R_{AH}/2M$  decreases monotonically as  $V$  goes from  $-1$  to  $1$ . Note that  $|V_{\text{extreme}}|$  is likely to be less than  $1$ , and also that the maximum & minimum values of  $R_{AH}$  do not have a simple relationship.

We have that  $R_{AH}/2M < 1$  where  $V > 0$ , i.e. where  $E' > 0$ . In other words, taking a  $(t, r)$  shell that intersects the AH at the fast pole, the light rays move fastest between the shells exactly where the shell is just emerging from the AH.

Some other features of the AH locus are discussed in appendix D.

## 8.3 Causal Structure of A Szekeres Wormhole

We shall next establish whether a radial null ray can pass through a Szekeres wormhole. We shall have to treat the neck separately from every other  $r$  value, because of the need to treat the  $f \rightarrow -1$  limit carefully.

### 8.3.1 Can $E' > 0$ Compensate for $M' > 0$ ?

As noted in [10] the introduction of matter into a wormhole slows the progress of light rays through it. Can this effect be compensated for by a suitable choice of  $E' > 0$ ? Since the vacuum case is  $M' = 0 = E'$ , for which we know the behaviour, we are only interested in the effects of varying  $M$  and  $E$ .

We start with the gradient of the null rays, eq (157) and use the substitutions (11) and (113) with (114) for  $R$ , &  $R'$  in terms of  $\eta$  &  $r$ , but we note that, if we choose the future AH — i.e. outgoing rays in a collapsing region — then

$$j = +1 \quad \text{and} \quad \pi < \eta \leq 2\pi. \quad (191)$$

So the gradient of the null rays in terms of  $\eta$  &  $r$  is

$$\begin{aligned} \left. \frac{dt}{dr} \right|_n &= \frac{1}{\sqrt{1+f}} \left( \frac{M(1-\cos\eta)}{(-f)\sqrt{1+f}} \right) \left\{ - \left( \frac{\sin\eta}{(1-\cos\eta)^2} \right) \frac{(-f)^{3/2}a'}{M} \right. \\ &\quad - \left( 1 - \frac{3\sin\eta(\eta-\sin\eta)}{2(1-\cos\eta)^2} \right) \frac{f'}{f} \\ &\quad \left. + \left( 1 - \frac{\sin\eta(\eta-\sin\eta)}{(1-\cos\eta)^2} \right) \frac{M'}{M} - \frac{E'}{E} \right\}. \end{aligned} \quad (192)$$

Consider a region in which  $R' > 0$  and  $M' > 0$ . Now since, in the above range of  $\eta$

$$\begin{aligned} 2 \geq 1 - \cos\eta \geq 0 \quad , \quad 0 \geq \frac{\sin\eta}{(1-\cos\eta)} \geq -\infty, \\ 1 \leq 1 - \frac{\sin\eta(\eta-\sin\eta)}{(1-\cos\eta)^2} \leq \infty \quad , \quad 1 \leq 1 - \frac{3\sin\eta(\eta-\sin\eta)}{2(1-\cos\eta)^2} \leq \infty, \end{aligned} \quad (193)$$

the coefficient of  $M'/M$  is always positive, and the coefficient of  $E'/E$  is always negative. In particular, because of the no shell crossing condition (97),  $|E'/E| \leq M'/3M$ , the  $E'/E$  term gives at most a partial cancellation of the  $M'/M$  term. Thus it is evident that varying  $E'/E$  cannot compensate for the effect of non-zero  $M'$  on the gradient of the radial rays.

We turn to the AH equation (163) with (161) and (191). We find the future AH equation in terms of  $\eta$  and  $r$  may be written

$$\begin{aligned} 0 &= \left[ 1 + \sqrt{\frac{(-f)}{(1+f)}} \frac{\sin\eta}{(1-\cos\eta)} \right] \left\{ \right. \\ &\quad - \frac{(-f)^{3/2}a'}{M} \left( \frac{\sin\eta}{(1-\cos\eta)^2} \right) - \frac{f'}{f} \left( 1 - \frac{3\sin\eta(\eta-\sin\eta)}{2(1-\cos\eta)^2} \right) \\ &\quad \left. + \frac{M'}{M} \left( 1 - \frac{\sin\eta(\eta-\sin\eta)}{(1-\cos\eta)^2} \right) \right\} - \left[ \sqrt{\frac{(-f)}{(1+f)}} \frac{\sin\eta}{(1-\cos\eta)} \right] \frac{E'}{E}. \end{aligned} \quad (194)$$

The solution is the parametric locus  $\eta = \eta_{AH}(r)$ . It is evident that if  $E' = 0$ , varying  $M'$  has no effect at all on the AH locus for a given  $M$ , as the solution is

$$\sqrt{\frac{(-f)}{(1+f)}} \frac{\sin\eta}{(1-\cos\eta)} = -1 \quad \Rightarrow \quad \cos\eta = 1 + 2f \quad \Rightarrow \quad R = 2M. \quad (195)$$

Similarly  $E'$  has no effect when  $\eta = \pi$ , and (see appendix D) when  $\eta = 0$  or  $2\pi$ . On the other hand, the effect of varying  $E'$  is influenced by the value of  $M'$ . Analysing the slope of this curve leads to pretty daunting expressions, but is fortunately not necessary.

Consider now the slope of a surface  $R(t, r) = \alpha M(r)$  in a collapsing region

$$R = \alpha M \quad \Rightarrow \quad \dot{R}^2 = \frac{2M}{\alpha M} + f \quad \Rightarrow \quad \left. \frac{dt}{dr} \right|_{R=\alpha M} = \frac{R' - \alpha M'}{\sqrt{\frac{2}{\alpha} + f}}, \quad (196)$$

where  $\alpha > 0$ . This is null or outgoing timelike wherever

$$\frac{(R' - \alpha M E' / E)}{\sqrt{1+f}} \leq \frac{R' - \alpha M'}{\sqrt{\frac{2}{\alpha} + f}}. \quad (197)$$

For  $M' = 0$ , which forces  $E' = 0$  (by eq. (97)), the equality obviously requires  $\alpha = 2$ , giving the event horizon in a vacuum model, and all  $R = \alpha M$  surfaces are outgoing timelike for  $\alpha > 2$ , and spacelike for  $\alpha < 2$ . For  $M' > 0$ , the condition  $E'/E < M'/3M$ , ensures the numerator of the lhs is no less than

$$R' - \alpha M' / 3. \quad (198)$$

For any given  $M' > 0$ ,  $R' > 0$  and  $f > -1$ , this is always greater than the numerator on the rhs, so, to satisfy the equality, the denominator on the lhs must be greater than that on the rhs, so once again

$$\alpha > 2. \quad (199)$$

Thus  $R = \alpha M$  surfaces can only be tangent to outgoing null rays for  $R = \alpha M > 2M$ , and for  $R < 2M$  they are spacelike, incoming null, or incoming timelike.

This allows us to conclude that, along the entire length of the future  $R = 2M$  surface, outgoing rays pass inside it, or run along it where  $M' = 0$ . By (11), the maximum  $R$  along any given constant  $r$  worldline in an elliptic region is at  $\eta = \pi$ , when

$$R_{max} = \frac{2M}{(-f)} \geq 2M, \quad (200)$$

while  $R$  grows without bound in parabolic and hyperbolic regions. Thus every particle worldline encounters the future  $R = 2M$  surface (and the past surface), leaving no room for any rays that arrive at the future  $R = 2M$  surface to escape to  $\mathcal{J}^+$ .

The time reverse of these arguments applies to the past AH, which lies in an expanding region and has incoming rays running along it or passing out of it.

To complete the argument, we must consider the limits at the neck,  $f \rightarrow -1$  where several derivatives are zero.

### 8.3.2 The AH at the Neck

Now we turn to consider the AH at the neck.

The differential of (161) with (163) and  $dp = 0 = dq$  gives us

$$\begin{aligned} 0 &= j \frac{\dot{R}}{\sqrt{1+f}} \left( R' - \frac{RE'}{E} \right) \left\{ \frac{\ddot{R} dt + \dot{R}' dr}{\dot{R}} - \frac{f' dr}{2(1+f)} \right. \\ &\quad \left. + \frac{\left( \dot{R}' dt + R'' dr - \frac{(\dot{R} dt + \dot{R}' dr)E'}{E} - \frac{RE'' dr}{E} + \frac{R(E')^2 dr}{E^2} \right)}{\left( R' - \frac{RE'}{E} \right)} \right\} \\ &\quad + \dot{R}' dt + R'' dr, \end{aligned} \quad (201)$$

$$\begin{aligned}
\left. \frac{dt}{dr} \right|_{AH} = & - \left\{ j \frac{\dot{R}'}{\sqrt{1+f}} \left( R' - \frac{RE'}{E} \right) - j \frac{\dot{R}f'}{2(1+f)^{3/2}} \left( R' - \frac{RE'}{E} \right) \right. \\
& \left. + j \frac{\dot{R}}{\sqrt{1+f}} \left( R'' - \frac{R'E'}{E} - \frac{RE''}{E} + \frac{R(E')^2}{E^2} \right) + R'' \right\} / \\
& \left[ j \frac{\ddot{R}}{\sqrt{1+f}} \left( R' - \frac{RE'}{E} \right) + j \frac{\dot{R}}{\sqrt{1+f}} \left( \dot{R}' - \frac{\dot{R}E'}{E} \right) + \dot{R}' \right]. \quad (202)
\end{aligned}$$

At the neck of the wormhole,  $r = r_n$ , the regularity conditions of sec. 6 give us the following limits, where  $L_{f'}$  etc are being defined in each case:

$$f \rightarrow -1, \quad (203)$$

$$f' \rightarrow 0, \quad f'/\sqrt{1+f} \rightarrow L_{f'} = 2f''/L_{f'} \geq 0 \Rightarrow (L_{f'})^2 = 2f'', \quad (204)$$

$$E' \rightarrow 0, \quad E'/\sqrt{1+f} \rightarrow L_{E'} = 2E''/L_{f'} \geq 0, \quad (205)$$

$$R' \rightarrow 0, \quad R'/\sqrt{1+f} \rightarrow L_{R'} = 2R''/L_{f'} > 0, \quad (206)$$

$$\dot{R}' \rightarrow 0, \quad \dot{R}'/\sqrt{1+f} \rightarrow L_{\dot{R}'} = 2\dot{R}''/L_{f'} = (\partial/\partial t)L_{R'}. \quad (207)$$

Thus the terms  $\dot{R}'R'/\sqrt{1+f}$ ,  $\dot{R}'RE'/E\sqrt{1+f}$ ,  $R'E'/E\sqrt{1+f}$ ,  $R(E')^2/E^2\sqrt{1+f}$  and  $\dot{R}'$ , go to zero and the remaining numerator terms involving  $\dot{R}$  cancel, down to

$$\left. \frac{dt}{dr} \right|_{AH,N} = -jR'' \left/ \left[ \frac{2\ddot{R}}{L_{f'}} \left( R'' - \frac{RE''}{E} \right) + \frac{\dot{R}}{\sqrt{1+f}} \left( \dot{R}' - \frac{\dot{R}E'}{E} \right) \right] \right., \quad (208)$$

$$\left. \frac{dt}{dr} \right|_{n,N} = j \frac{2(R'' - RE''/E)}{L_{f'}}. \quad (209)$$

Since the AH only intersects the neck when  $\dot{R} = 0$ , the behaviour of  $\dot{R}/\sqrt{1+f}$  and  $\dot{R}^2/\sqrt{1+f}$  must still be determined (and that of  $\dot{R}'$  will be verified).

At the moment of maximum expansion in the neck we have

$$R = 2M, \quad \dot{R} = 0, \quad \sqrt{1+f} = 0, \quad (210)$$

$$\eta = \pi, \quad \cos \eta = -1, \quad \sin \eta = 0, \quad (211)$$

and so, using

$$\begin{aligned}
R' = & \frac{M}{(-f)} \left\{ \left( \frac{M'}{M} - \frac{f'}{f} \right) (1 - \cos \eta) - \left( \frac{M'}{M} - \frac{3f'}{2f} \right) \frac{\sin \eta(\eta - \sin \eta)}{(1 - \cos \eta)} \right\} \\
& - a' \sqrt{-f} \frac{\sin \eta}{(1 - \cos \eta)}, \quad (212)
\end{aligned}$$

$$\begin{aligned}
R'' = & \frac{-1}{(1 - \cos \eta)^2} \frac{M}{(-f)} \left\{ (\eta - \sin \eta) \left( \frac{M'}{M} - \frac{3f'}{2f} \right) + \frac{a'(-f)^{3/2}}{M} \right\}^2 \\
& + \frac{\sin \eta}{(1 - \cos \eta)} \left\{ (\eta - \sin \eta) \frac{M}{(-f)} \left[ \frac{2f'}{f} \left( \frac{M'}{M} - \frac{9f'}{8f} \right) - \left( \frac{M''}{M} - \frac{3f''}{2f} \right) \right] \right. \\
& \left. - \sqrt{-f} \left( a'' + a' \frac{f'}{f} \right) \right\} + (1 - \cos \eta) \frac{M}{(-f)} \left\{ \frac{M''}{M} - \frac{f''}{f} - \frac{2f'}{f} \left( \frac{M'}{M} - \frac{f'}{f} \right) \right\} \quad (213)
\end{aligned}$$

gives, by virtue of (204) and (140):

$$L_{R'} = 2(L_{M'} + ML_{f'}) = 4(M'' + Mf'')/L_{f'} \quad , \quad R'' = 2(M'' + Mf''). \quad (214)$$

We find the limit of  $\dot{R}/\sqrt{1+f}$  at this point by combining (161) and (163), to obtain

$$\frac{\dot{R}}{\sqrt{1+f}} \Big|_{\text{MEN}} = \frac{-jL_{R'}}{L_{R'} - RL_{E'}/E} = \frac{-j(M'' + Mf'')}{M'' + Mf'' - ME''/E}, \quad (215)$$

so it is clear that  $\dot{R}^2 E'/\sqrt{1+f} = 0$ . To check the limit of  $\dot{R}'$ , the  $r$  derivative of (4) gives

$$\dot{R}' = \frac{1}{\dot{R}} \left( \frac{M'}{R} - \frac{MR'}{R^2} + \frac{f'}{2} \right) \quad \rightarrow \quad \frac{\dot{R}\dot{R}'}{\sqrt{1+f}} = \left( \frac{L_{M'}}{R} - \frac{ML_{R'}}{R^2} + \frac{L_{f'}}{2} \right), \quad (216)$$

and because of (214) and  $R = 2M$  all terms in the bracket cancel, verifying that  $\dot{R}\dot{R}'/\sqrt{1+f} = 0$ .

These together with (5) give us

$$\frac{dt}{dr} \Big|_{AH,\text{MEN}} = j \frac{4Mf''(M'' + Mf'')}{L_{f'}(M'' + Mf'' - ME''/E)}, \quad (217)$$

$$\frac{dt}{dr} \Big|_{n,\text{MEN}} = j \frac{4(M'' + Mf'' - ME''/E)}{L_{f'}}. \quad (218)$$

For a light ray to pass through the neck at the moment of maximum expansion without falling inside the AH, we need  $dt/dr|_{AH,\text{MEN}} > dt/dr|_{n,\text{MEN}}$ , in other words

$$\frac{dt/dr|_{AH,\text{MEN}}}{dt/dr|_{n,\text{MEN}}} = \frac{Mf''(M'' + Mf'')}{(M'' + Mf'' - ME''/E)^2} \Big|_{\text{MEN}} > 1, \quad (219)$$

or

$$\frac{(M'' + Mf'') - \sqrt{Mf''(M'' + Mf'')}}{M} < \frac{E''}{E} < \frac{(M'' + Mf'') + \sqrt{Mf''(M'' + Mf'')}}{M}. \quad (220)$$

Since  $M(r)$  is positive, and both  $M(r)$  and  $f(r)$  are at a minimum at the neck, i.e.  $M'' > 0$  &  $f'' > 0$ , we have  $\sqrt{Mf''(M'' + Mf'')} < M'' + Mf''$ , and so both upper and lower limits are real and positive.

Can this requirement be satisfied without creating shell crossings? The only relevant condition is the one for  $\epsilon = +1$ ,  $R' = 0$ ,  $f = -1$ ,  $R'' > 0$

$$\frac{E''}{E} \Big|_{\text{max}} \leq \frac{M''}{3M}. \quad (221)$$

To be able to satisfy this as well as (220) we would need

$$\frac{M'' + Mf'' - \sqrt{Mf''(M'' + Mf'')}}{M} < \frac{M''}{3M}, \quad (222)$$

but this leads to

$$M''(4M'' + 3Mf'') < 0, \quad (223)$$

which is clearly not possible. Indeed, although  $\rho$  is zero rather than divergent where  $E'/E = M'/3M$ , where  $E'/E$  exceeds  $M'/3M$ , the density is negative at all times.

Putting the maximum value,  $E''/E = M''/3M$  into (219) gives

$$\left. \frac{dt/dr|_{AH,MEN}}{dt/dr|_{n,MEN}} \right|_{\max} = \frac{9Mf''(M'' + Mf'')}{(2M'' + 3Mf'')^2}, \quad (224)$$

which rises from 0 at  $f''/M'' = 0$ , and asymptotically approaches 1 as  $f''/M'' \rightarrow \infty$ , i.e. vacuum.

Therefore, even at the neck,  $E' > 0$  cannot compensate for  $M' > 0$ , and all rays passing through this event remain within  $R \leq 2M$ , passing from inside  $AH^-$  to inside  $AH^+$ .

### 8.3.3 Summary

In a Szekeres wormhole, every particle worldline encounters  $R = 2M$ , twice for most  $r$  values and once where  $f = -1$ , making this a pair of 3-surfaces that span the spacetime. The apparent horizons coincide with  $R = 2M$  at an extremum of  $R(t = \text{const}, r)$  — a neck or belly — where  $f = -1$ . Where  $M' = 0$  (vacuum), the  $R = 2M$  surfaces are (locally) null.

Assuming there is matter ( $M' > 0$ ) somewhere within the elliptic region describing the neck, and assuming the two regions,  $r \rightarrow \pm\infty$ , are asymptotically flat, i.e.  $M \rightarrow M_{\text{tot}} = \text{constant}$  ( $E' \rightarrow 0$ ), then the event horizon is the set of rays that are asymptotic to  $R = 2M$ , but always lie outside. The future event horizon  $EH^+$  emerges from  $R = 2M$  surface, and vice-versa for  $EH^-$ .

Thus we conclude that the causal structure of a regular Szekeres wormhole is only a quantitative modification of the LT wormhole (dense black hole), and the possible causal diagrams for Szekeres models are essentially the same as those for LT models, as given in [10].

### 8.3.4 Numerical Examples

A few numerical examples were produced as follows.

We choose the 3 LT arbitrary functions to produce a Kruskal-like topology, with the neck at  $r = 0$ , that is mirror symmetric about  $r = 0$  and  $t = 0$ . The choice must therefore satisfy  $f(0) = -1$ ,  $f'(0) = 0$ ,  $f''(0) > 0$ ,  $M'(0) = 0$ ,  $M''(0) > 0$ ,  $a(r) = -b(r)$ ;

$$M = M_0(1 + M_1r^2)^3, \quad M_0, M_1 > 0, \quad (225)$$

$$f = -\exp(-r^2/r_s), \quad r_s > 0, \quad (226)$$

$$a = -\pi M/(-f)^{3/2}. \quad (227)$$

We want to choose  $E$  to maximise the effect of  $E' \neq 0$  along one particular radial path. By setting

$$P(r) = 0 = Q(r), \quad (228)$$

so that (13) is

$$E = \frac{S}{2} \left( \frac{p^2}{S^2} + \frac{q^2}{S^2} + 1 \right), \quad (229)$$

the maximum  $E'/E$  becomes

$$\left| \frac{E'}{E} \right|_{max} = \left| \frac{S'}{S} \right| \quad (230)$$

along the direction  $(p, q) = (0, 0)$ , i.e.  $\theta = 0$ . Since numerical integrations will only be done along this path and the  $\theta = \pi$  one, we treat  $E$  as a function of  $r$  only. We make  $E'/E$  as large as possible without violating the no shell crossings condition  $E'/E \leq M'/3M$  with

$$E = E_0(1 + E_1 r^2) + E_2, \quad E_0, E_1, E_2 > 0, \quad (231)$$

where the shell crossing occurs somewhere if  $E_2 = 0$ .

Because of the two reflection symmetries, we can start integrating a null ray from maximum expansion at the neck,

$$\eta = \pi, \quad r = 0, \quad (232)$$

where AH<sup>+</sup> & AH<sup>-</sup> meet. The symmetry means that integrating forwards along increasing  $r$  &  $t$  and integrating backwards along decreasing  $r$  &  $t$  is the same thing, so one integration actually traces both halves of the same ray. Rays that don't pass through this point require two separate parts to the integration, one from maximum expansion towards  $r$  &  $t$  increasing, and the other towards  $r$  &  $t$  decreasing, with careful treatment of the neck limits where  $r$  goes through zero.

The following runs were done:

- Test 1 — the vacuum case:

$$M_0 = 1, \quad M_1 = 0, \quad E_0 = 1, \quad E_1 = 0, \quad E_2 = 0, \quad r_s = 1. \quad (233)$$

As expected, we found that the fast AH, the slow AH, the fast null ray, and the slow null ray were all the same.

- Test 2 — the LT case:

$$M_0 = 1, \quad M_1 = 0.1, \quad E_0 = 1, \quad E_1 = 0, \quad E_2 = 0.01, \quad r_s = 1. \quad (234)$$

Here the fast & slow rays were the same, and the fast & slow AHs were the same, but the rays fell inside the AHs, as expected.

- Test 3 — a Szekeres version of above LT case:

$$M_0 = 1, \quad M_1 = 0.1, \quad E_0 = 1, \quad E_1 = 0.1, \quad E_2 = 0.01, \quad r_s = 1. \quad (235)$$

The AHs and rays were split on either side of the Test 2 curves.

- Run 1 — medium  $M'/f'$

$$M_0 = 1, \quad M_1 = 1, \quad E_0 = 1, \quad E_1 = 1, \quad E_2 = 0, \quad r_s = 1. \quad (236)$$

We found that the rays & AHs were well split, while the rays were strongly trapped.

- Run 2 — low  $M'/f'$

$$M_0 = 1, \quad M_1 = 1, \quad E_0 = 1, \quad E_1 = 1, \quad E_2 = 0.1, \quad r_s = 0.01. \quad (237)$$

The rays were mildly split, the AHs were indistinguishable in the range plotted, and the rays were mildly trapped.

- Run 3 — slightly less low  $M'/f'$

$$M_0 = 1, \quad M_1 = 2, \quad E_0 = 1, \quad E_1 = 2, \quad E_2 = 0.01, \quad r_s = 0.01. \quad (238)$$

This was very similar to the previous run, with the rays less mildly trapped.

- Run 4 — high  $M'/f'$

$$M_0 = 1, \quad M_1 = 2, \quad E_0 = 1, \quad E_1 = 2, \quad E_2 = 0.01, \quad r_s = 0.01. \quad (239)$$

Here the rays & AHs were well split, and the rays were very strongly trapped.

These examples cover the main possibilites, and run 1 is shown in Fig. 6.

## 9 Conclusions

Szekeres (S) models are a generalisation of the spherically symmetric Lemaître-Tolman (LT) models. Both describe inhomogeneous dust distributions, but the former have no Killing vectors. There are 3 arbitrary functions of coordinate radius in LT models ( $M$ ,  $f$  &  $a$ ), and a further 3 in S models ( $S$ ,  $P$  &  $Q$ ).

For quasi-spherical Szekeres (S) models, we established 3 sets of regularity conditions — the conditions for a regular origin, the conditions for no shell crossings, and the conditions for regular maxima and minima in the spatial sections. The last two contain exactly those for the LT models, with extra conditions on the arbitrary functions that are peculiar to S. Thus, for every regular LT model that is non-vacuum ( $M' > 0$ ) at least somewhere, one can find regular S models that are anisotropic versions of the same topology. (For vacuum,  $M' = 0$ , S models must be spherically symmetric.)

Since LT models can reproduce the Schwarzschild-Kruskal-Szekeres topology of a wormhole connecting two universes, but with non-zero density everywhere, this is also possible with S models. In the vacuum case ( $M' = 0$ ) this gives the full Kruskal manifold in geodesic coordinates. It is known that the presence of matter in such models inhibits communication through the wormhole and splits the event horizons. We investigated the S wormhole models, considering apparent horizons and the paths of ‘radial’ null rays, which, while not geodesic, are the fastest paths out of a wormhole. We showed that, even though the S model’s anisotropy makes the proper separation of consecutive shells shorter along certain directions, and null motion faster along those same directions, this is not enough to compensate for the retarding effect of matter. Thus the causal structure of an S wormhole is the same as that of the corresponding LT model.

We also considered whether the two universes on either side of a wormhole could be joined across a 3-surface, making a handle topology. It was found that a smooth junction is not possible at any finite distance, as a surface layer would be created. This conclusion applies to LT models and to the vacuum case — a Schwarzschild wormhole — too.

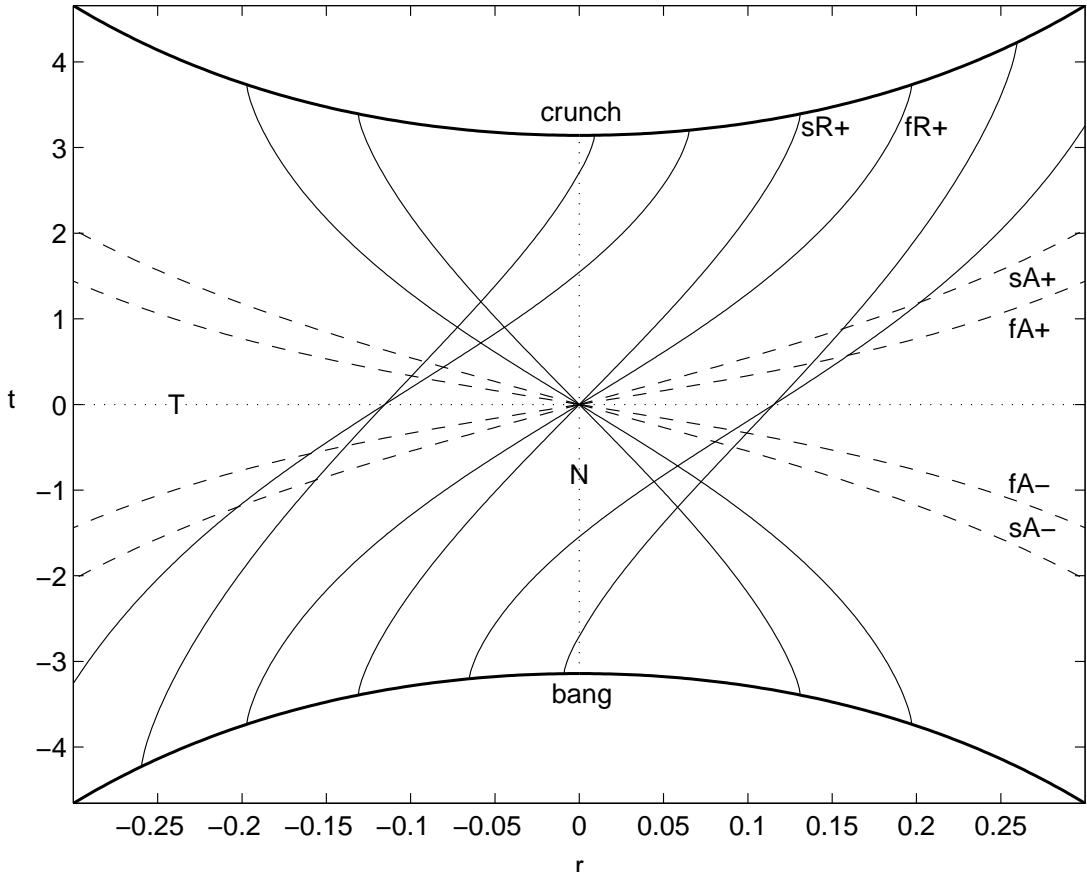


Figure 6: The  $(r - t)$  diagram for the Szekeres model defined for run 1, showing the fast and slow future apparent horizons ( $fA+$  and  $sA+$ ), and past apparent horizons, the fast and slow rays that pass through  $O$  — the neck at the moment of maximum expansion — towards  $r$  increasing ( $fR+$  and  $sR+$ ), and rays through  $O$  going towards  $r$  decreasing, as well as rays going through other points.  $T$  is the moment of time symmetry which is also the simultaneous time of maximum expansion, and  $N$  is the locus of the neck  $r = 0$ . Note that  $fA+$  &  $sA+$  are two different intersections of the future apparent horizon  $AH^+$  in two different radial directions — the fast & slow poles where  $E'/E$  takes extreme values. Note also that there is no origin  $R(r = r_o, t) = 0$  in wormhole models.

## Acknowledgments

## References

- [1] A. Barnes (1970) *J. Phys* **A3**, 653-661.
- [2] B.K. Berger, D.M. Eardley and D. W. Olson (1977) *Phys. Rev. D* **16**, 3086-9.
- [3] W.B. Bonnor (1976a) *Nature* **263**, 301.
- [4] W.B. Bonnor (1976b) *Comm. Math. Phys.* **51**, 191-9.
- [5] W.B. Bonnor (1997) *Mathematical Reviews* **97 g 83 026** (July 1997, p 4592).
- [6] W.B. Bonnor, A.H. Sulaiman and N. Tomimura (1977), *Gen. Rel. Grav.* **8**, 549-559.
- [7] W. B. Bonnor, N. Tomimura (1976), *Mon. Not. Roy. Astr. Soc.* **175**, 85.
- [8] B. Datt (1938), *Z. Physik* **108**, 314; reprinted in *Gen. Rel. Grav.* **31**, 1619 (1999).
- [9] M.M. de Souza (1985) *Rev. Bras. Fiz.* **15**, 379.
- [10] C. Hellaby (1987) *Class. Q. Grav.* **4**, 635-50.
- [11] C. Hellaby (1996) *Class. Q. Grav.* **13**, 2537-46.
- [12] C. Hellaby (1996) *J. Math. Phys.* **37**, 2892-905.
- [13] C. Hellaby and K. Lake (1985) *Astrophys. J.* **290**, 381-7.
- [14] W. Kinnersley (1969) *Phys. Rev.* **186**, 1335-6.
- [15] D. Kramer, H. Stephani, E. Herlt and M.A.H. MacCallum (1980) *Exact Solutions of Einstein's Field Equations*, Cambridge U P, ISBN 0 521 23041 1.
- [16] A. Krasiński (1989) *J. Math. Phys.*, **30**, 433-441.
- [17] A. Krasiński (1997) *Inhomogeneous Cosmological Models*, Cambridge U P, ISBN 0 521 48180 5.
- [18] M. Kruskal (1960) *Phys. Rev.*, **119**, 1743-1745.
- [19] G. Lemaître (1933) *Ann. Soc. Sci. Bruxelles* **A53** 51-85; reprinted in *Gen. Rel. Grav.* **29**, 641-80 (1997).
- [20] P. Musgrave, D. Pollney and K. Lake (1996), GRTensorII release 1.50, and GRJunction 2.0, running under Maple V release 3; and GRTensorII release 1.76, running under Maple V release 5. (Physics Department, Queen's University, Kingston, Ontario, K7L 3N6, CANADA; E-mail: [grtensor@astro.queensu.ca](mailto:grtensor@astro.queensu.ca).)
- [21] V. A. Ruban (1968), *Pisma v Red. ZhETF* **8**, 669 [*Sov. Phys. JETP Lett.* **8**, 414 (1968)]; reprinted in *Gen. Rel. Grav.* **33**, 369 (2001).

- [22] V. A. Ruban (1969), *ZhETF* **56**, 1914 [Sov. Phys. *JETP* **29**, 1027 (1969)]; reprinted in *Gen. Rel. Grav.* **33**, 375 (2001).
- [23] G. Szekeres (1960) *Publicationes Mathematicae Debrecen* **7**, 285-301; reprinted in *Gen. Rel. Grav.* **34**, xxx (2002).
- [24] P. Szekeres (1975a) *Comm. Math. Phys.* **41**, 55-64.
- [25] P. Szekeres (1975b) *Phys. Rev. D* **12**, 2941-8.
- [26] R.C. Tolman (1934) *Proc. Nat. Acad. Sci.* **20** 169-76, reprinted in *Gen. Rel. Grav.* **29**, 935-43 (1997).

## A The hypersurface of zero mass-dipole intersects every $(t = \text{const}, r = \text{const})$ sphere.

This hypersurface is given by

$$E'/E = (A' + C')/(A + C). \quad (240)$$

Since  $E'/E$  at constant  $r$  is bounded (see (64)), it must be verified whether eq. (240) has a solution in every sphere of constant  $t$  and  $r$ . The solution will exist when

$$(E'/E)_{\min} \leq (A' + C')/(A + C) \leq (E'/E)_{\max}. \quad (241)$$

Since  $(E'/E)_{\min} = -(E'/E)_{\max}$ , eq. (241) is equivalent to

$$(A' + C')^2/(A + C)^2 \leq (E'/E)_{\text{extreme}}^2 = \frac{1}{S^2} (P'^2 + Q'^2 + S'^2). \quad (242)$$

We have

$$\begin{aligned} A + C &= \frac{1}{2S} (1 + P^2 + Q^2 + S^2) \\ A' + C' &= \frac{S'}{2S^2} (S^2 - P^2 - Q^2 - 1) + \frac{1}{S} (PP' + QQ'). \end{aligned} \quad (243)$$

Substituted in (242), this leads to

$$\begin{aligned} 4S^2S'^2(1 + P^2 + Q^2) - 4SS'(PP' + QQ')(S^2 - P^2 - Q^2 - 1) \\ - 4S^2(PP' + QQ')^2 + (P'^2 + Q'^2)(1 + P^2 + Q^2 + S^2) \geq 0. \end{aligned} \quad (244)$$

The discriminant of this with respect to  $S'$  is

$$\Delta = -16S^2(1 + P^2 + Q^2 + S^2)^2 [(PQ' - QP')^2 + P'^2 + Q'^2], \quad (245)$$

and is always negative unless  $P' = Q' = 0$ . This means that with  $P' \neq 0 \neq Q'$ , the l.h.s. of (244) is strictly positive. Even when  $P' = Q' = 0$ , it is still strictly positive unless  $S' = 0$  as well. However,  $P' = Q' = S' = 0$  implies  $A' = C' = 0$  and  $E' = 0$  on the whole sphere, and

then the dipole component of density  $\Delta\rho = 0$ ; i.e. on such a sphere the density is spherically symmetric. Hence, apart from the spherically symmetric subcase, eq. (241) is fulfilled, with sharp inequalities in both places. This means that the  $\Delta\rho = 0$  hypersurface intersects every  $(t = \text{const}, r = \text{const})$  sphere along a circle parallel to the  $E' = 0$  circle (see remark after eq. (58)).

## B Matching the Szekeres Metric to Itself

We here lay out the calculations necessary for matching the Szekeres metric across a comoving surface to some other metric, and in particular to another Szekeres metric.

Given a comoving surface,

$$r_\Sigma = Z(p, q) \quad (246)$$

and surface coordinates,

$$\xi^i = (t, p, q) \quad (247)$$

we calculate the basis vectors in the surface,

$$e_i^\mu = \frac{\partial x_\pm^\mu}{\partial \xi^i}, \quad (248)$$

the 1st fundamental form,

$${}^3g_{ij}^+ = {}^3g_{ij}^- = g_{\mu\nu}^\pm e_i^\mu e_j^\nu, \quad (249)$$

the normal vector,

$$n_\mu, \quad n_\mu n^\mu = 1, \quad n_\mu e_i^\mu = 0, \quad (250)$$

and the 2nd fundamental form

$$K_{ij}^\pm = -n_\lambda^\pm \left( \frac{\partial^2 x^\lambda}{\partial \xi^i \partial \xi^j} + \Gamma_{\mu\nu}^\lambda \frac{\partial x^\mu}{\partial \xi^i} \frac{\partial x^\nu}{\partial \xi^j} \right). \quad (251)$$

Using GRTensor/GRJunction [20] we find the following for the intrinsic metric:

$${}^3g_{tt} = -1, \quad (252)$$

$${}^3g_{pp} = \frac{Z_p^2 (R' - RE'/E)^2 E^2 + R^2(\epsilon + f)}{E^2(\epsilon + f)}, \quad (253)$$

$${}^3g_{pq} = \frac{Z_p Z_q (R' - RE'/E)^2}{(\epsilon + f)}, \quad (254)$$

$${}^3g_{qq} = \frac{Z_q^2 (R' - RE'/E)^2 E^2 + R^2(\epsilon + f)}{E^2(\epsilon + f)}, \quad (255)$$

the surface basis vectors:

$$e_i^t = (1, 0, 0), \quad (256)$$

$$e_i^r = (0, Z_p, Z_q), \quad (257)$$

$$e_i^p = (0, 1, 0), \quad (258)$$

$$e_i^q = (0, 0, 1), \quad (259)$$

$$(260)$$

the surface normal:

$$n_r = -\frac{(R'E - RE')R}{E\Delta}, \quad (261)$$

$$n_p = \frac{Z_p(R'E - RE')R}{E\Delta}, \quad (262)$$

$$n_q = \frac{Z_q(R'E - RE')R}{E\Delta}, \quad (263)$$

$$\text{where } Z_p = \frac{\partial Z}{\partial p} \quad , \quad Z_q = \frac{\partial Z}{\partial q} \quad , \quad (264)$$

$$\Delta = \left( R^2(\epsilon + f) + (Z_p^2 + Z_q^2)(R'E - RE')^2 \right)^{1/2}, \quad (265)$$

and the extrinsic curvature:

$$K_{pt} = \frac{[Z_p(R\dot{R}' - \dot{R}R')]}{\Delta}, \quad (266)$$

$$K_{qt} = \frac{[Z_q(R\dot{R}' - \dot{R}R')]}{\Delta}, \quad (267)$$

$$\begin{aligned} K_{pp} = & \frac{1}{2E^2(\epsilon + f)\Delta} [2RE(R'E - RE')(\epsilon + f)Z_{pp} \\ & + 2(R'E - RE')^2(E_pE' - E'_pE)Z_p^3 \\ & + 2(R'E - RE')^2(E_qE' - E'_qE)Z_p^2Z_q \\ & + (2\{3ER'RE' + RR''E^2 - (E')^2R^2 - 2E^2(R')^2 - R^2E''E\}(\epsilon + f) \\ & - Rf'E(R'E - RE'))Z_p^2 \\ & - 2R(2RE'_pE - E_pR'E - RE_pE')(\epsilon + f)Z_p \\ & - 2RE_q(R'E - RE')(\epsilon + f)Z_q \\ & - 2R^2(\epsilon + f)^2], \end{aligned} \quad (268)$$

$$\begin{aligned} K_{pq} = & \frac{1}{2E^2(\epsilon + f)\Delta} [2RE(R'E - RE')(\epsilon + f)Z_{pq} \\ & + 2(R'E - RE')^2(E_pE' - E'_pE)Z_p^2Z_q \\ & + 2(R'E - RE')^2(E_qE' - E'_qE)Z_pZ_q^2 \\ & + (2\{3ER'RE' + RR''E^2 - (E')^2R^2 - 2E^2(R')^2 - R^2E''E\}(\epsilon + f) \\ & - Rf'E(R'E - RE'))Z_pZ_q \\ & - 2RE(RE'_q - R'E_q)(\epsilon + f)Z_p \\ & - 2RE(RE'_p - R'E_p)(\epsilon + f)Z_q], \end{aligned} \quad (269)$$

$$\begin{aligned} K_{qq} = & \frac{1}{2E^2(\epsilon + f)\Delta} [2RE(R'E - RE')(\epsilon + f)Z_{qq} \\ & + 2(R'E - RE')^2(E_pE' - E'_pE)Z_pZ_q^2 \end{aligned}$$

$$\begin{aligned}
& + 2(R'E - RE')^2(E_q E' - E'_q E)Z_q^3 \\
& + (2\{3ER'RE' + RR''E^2 - (E')^2R^2 - 2E^2(R')^2 - R^2E''E\}(\epsilon + f) \\
& \quad - Rf'E(R'E - RE'))Z_q^2 \\
& - 2RE_p(R'E - RE')(\epsilon + f)Z_p \\
& - 2R(2RE'_q E - E_q R'E - RE_q E')(\epsilon + f)Z_q \\
& - 2R^2(\epsilon + f)^2],
\end{aligned} \tag{270}$$

where all quantities are evaluated on  $\Sigma$ .

## C The Acceleration of a Given Tangent Vector

Starting from

$$a^\alpha = k^\beta \nabla_\beta k^\alpha = k^\beta \partial_\beta k^\alpha + \Gamma^\alpha_{\beta\gamma} k^\beta k^\gamma, \tag{271}$$

the individual acceleration components for a given  $k^\alpha$  in the Szekeres metric are

$$\begin{aligned}
a^t &= k^\beta \partial_\beta k^t + \Gamma^t_{rr}(k^r)^2 + \Gamma^t_{pp}(k^p)^2 + \Gamma^t_{qq}(k^q)^2 \\
&= k^t \partial_t k^t + k^r \partial_r k^t + k^p \partial_p k^t + k^q \partial_q k^t
\end{aligned} \tag{272}$$

$$+ \left( R' - \frac{RE'}{E} \right) \left( \dot{R}' - \frac{\dot{R}E'}{E} \right) \frac{1}{\epsilon + f} (k^r)^2 + \left( \frac{R\dot{R}}{E^2} \right) ((k^p)^2 + (k^q)^2), \tag{273}$$

$$\begin{aligned}
a^r &= k^\beta \partial_\beta k^r + 2\Gamma^r_{tr} k^t k^r + \Gamma^r_{rr}(k^r)^2 + 2\Gamma^r_{rp} k^r k^p + 2\Gamma^r_{rq} k^r k^q \\
&\quad + \Gamma^r_{pp}(k^p)^2 + \Gamma^r_{qq}(k^q)^2
\end{aligned} \tag{274}$$

$$\begin{aligned}
&= k^t \partial_t k^r + k^r \partial_r k^r + k^p \partial_p k^r + k^q \partial_q k^r + \frac{2 \left( \dot{R}' - \frac{\dot{R}E'}{E} \right)}{\left( R' - \frac{RE'}{E} \right)} k^t k^r \\
&\quad + \left[ \frac{\left( R' - \frac{RE'}{E} \right)'}{\left( R' - \frac{RE'}{E} \right)} - \frac{f'}{2(\epsilon + f)} \right] (k^r)^2 - \frac{2R \left( \frac{E'_p}{E} - \frac{E'E_p}{E^2} \right)}{\left( R' - \frac{RE'}{E} \right)} k^r k^p \\
&\quad - \frac{2R \left( \frac{E'_q}{E} - \frac{E'E_q}{E^2} \right)}{\left( R' - \frac{RE'}{E} \right)} k^r k^q - \frac{R(\epsilon + f)}{E^2 \left( R' - \frac{RE'}{E} \right)} ((k^p)^2 + (k^q)^2),
\end{aligned} \tag{275}$$

$$\begin{aligned}
a^p &= k^\beta \partial_\beta k^p + 2\Gamma^p_{tp} k^t k^p + \Gamma^p_{rr}(k^r)^2 + 2\Gamma^p_{rp} k^r k^p \\
&\quad + \Gamma^p_{pp}(k^p)^2 + 2\Gamma^p_{pq} k^p k^q + \Gamma^p_{qq}(k^q)^2
\end{aligned} \tag{276}$$

$$\begin{aligned}
&= k^t \partial_t k^p + k^r \partial_r k^p + k^p \partial_p k^p + k^q \partial_q k^p + \frac{2\dot{R}}{R} k^t k^p \\
&\quad - \frac{\left( R' - \frac{RE'}{E} \right) (EE'_p - E'E_p)}{R(\epsilon + f)} (k^r)^2 + \frac{2 \left( R' - \frac{RE'}{E} \right)}{R} k^r k^p
\end{aligned}$$

$$-\frac{E_p}{E}(k^p)^2 - \frac{2E_q}{E}k^p k^q + \frac{E_p}{E}(k^q)^2, \quad (277)$$

$$\begin{aligned} a^q &= k^\beta \partial_\beta k^q + 2\Gamma^q_{tq} k^t k^q + \Gamma^q_{rr} (k^r)^2 + 2\Gamma^q_{rq} k^r k^q \\ &\quad + \Gamma^q_{pp} (k^p)^2 + 2\Gamma^q_{pq} k^p k^q + \Gamma^q_{qq} (k^q)^2 \end{aligned} \quad (278)$$

$$\begin{aligned} &= k^t \partial_t k^q + k^r \partial_r k^q + k^p \partial_p k^q + k^q \partial_q k^q + \frac{2\dot{R}}{R} k^t k^q \\ &\quad - \frac{\left(R' - \frac{RE'}{E}\right) (EE'_q - E'E_q)}{R(\epsilon + f)} (k^r)^2 + \frac{2\left(R' - \frac{RE'}{E}\right)}{R} k^r k^q \\ &\quad + \frac{E_q}{E} (k^p)^2 - \frac{2E_p}{E} k^p k^q - \frac{E_q}{E} (k^q)^2. \end{aligned} \quad (279)$$

For “radial” paths  $k^p = 0 = k^q$ ,  $\partial_p k^\alpha = 0 = \partial_q k^\alpha$  these reduce to

$$\begin{aligned} a^t &= k^t \partial_t k^t + k^r \partial_r k^t \\ &\quad + \left(R' - \frac{RE'}{E}\right) \left(\dot{R}' - \frac{\dot{R}E'}{E}\right) \frac{1}{(\epsilon + f)} (k^r)^2, \end{aligned} \quad (280)$$

$$\begin{aligned} a^r &= k^t \partial_t k^r + k^r \partial_r k^r + \frac{2\left(\dot{R}' - \frac{\dot{R}E'}{E}\right)}{\left(R' - \frac{RE'}{E}\right)} k^t k^r \\ &\quad + \left[ \frac{\left(R' - \frac{RE'}{E}\right)'}{\left(R' - \frac{RE'}{E}\right)} - \frac{f'}{2(\epsilon + f)} \right] (k^r)^2, \end{aligned} \quad (281)$$

$$a^p = -\frac{\left(R' - \frac{RE'}{E}\right) (EE'_p - E'E_p)}{R(\epsilon + f)} (k^r)^2, \quad (282)$$

$$a^q = -\frac{\left(R' - \frac{RE'}{E}\right) (EE'_q - E'E_q)}{R(\epsilon + f)} (k^r)^2. \quad (283)$$

Using the “radial” null condition

$$k^t = \frac{jk^r}{\sqrt{\epsilon + f}} \left(R' - \frac{RE'}{E}\right) \quad (284)$$

the acceleration becomes

$$\begin{aligned} a^t &= \frac{j}{\sqrt{\epsilon + f}} \left\{ \left(\dot{R}' - \frac{\dot{R}E'}{E}\right) k^t k^r + \left(R' - \frac{RE'}{E}\right) k^t \partial_t k^r \right\} \\ &\quad + \frac{j}{\sqrt{\epsilon + f}} \left\{ \left[ \left(R' - \frac{RE'}{E}\right)' - \frac{f'}{2(\epsilon + f)} \left(R' - \frac{RE'}{E}\right) \right] (k^r)^2 \right. \\ &\quad \left. + \left(R' - \frac{RE'}{E}\right) k^r \partial_r k^r \right\} + \left(R' - \frac{RE'}{E}\right) \left(\dot{R}' - \frac{\dot{R}E'}{E}\right) \frac{1}{(\epsilon + f)} (k^r)^2, \end{aligned} \quad (285)$$

$$a^r = k^r \partial_r k^r + \frac{j}{\sqrt{\epsilon + f}} \left\{ \left( R' - \frac{RE'}{E} \right) k^r \partial_t k^r + 2 \left( \dot{R}' - \frac{\dot{R}E'}{E} \right) (k^r)^2 \right\} \\ + \left[ \frac{\left( R' - \frac{RE'}{E} \right)'}{\left( R' - \frac{RE'}{E} \right)} - \frac{f'}{2(\epsilon + f)} \right] (k^r)^2, \quad (286)$$

$$a^p = -\frac{\left( R' - \frac{RE'}{E} \right) (EE'_p - E'E_p)}{R(\epsilon + f)} (k^r)^2, \quad (287)$$

$$a^q = -\frac{\left( R' - \frac{RE'}{E} \right) (EE'_q - E'E_q)}{R(\epsilon + f)} (k^r)^2. \quad (288)$$

While  $E' = 0$  gives the expected LT values, we note that  $E(r, p, q)$  determines whether  $a^p$  and  $a^q$  are zero or not.

In the  $\epsilon = +1$  case, by (16), (60) and (62), the extremes of  $E$  on a given 2-sphere are located at

$$p_e = P + \frac{P'S}{\left( \pm \sqrt{(S')^2 + (P')^2 + (Q')^2} - S' \right)} \quad (289)$$

$$q_e = Q + \frac{Q'S}{\left( \pm \sqrt{(S')^2 + (P')^2 + (Q')^2} - S' \right)} \quad (290)$$

and it is easily verified that  $a^p = 0 = a^q$  in these two antipodal directions. It follows that initially radial geodesics in these directions remain radial if  $p_e$  &  $q_e$  are constant with  $r$ . For example, if  $p_e = 0 = q_e$ , this would require arbitrary functions satisfying

$$\frac{P'}{P} = \frac{2S'S}{S^2 - P^2 - Q^2} = \frac{Q'}{Q} \quad (291)$$

$$\text{or} \quad P = 0, \quad \frac{Q'}{Q} = \frac{2S'S}{S^2 - Q^2}, \quad \text{when } P' = 0 \quad (292)$$

$$\text{or} \quad \frac{P'}{P} = \frac{2S'S}{S^2 - P^2}, \quad Q = 0, \quad \text{when } Q' = 0 \quad (293)$$

$$\text{or} \quad P = 0, \quad Q = 0, \quad \text{when } P' = 0 \quad \text{and} \quad Q' = 0 \quad (294)$$

## D Other Features of the AH

### The FLRW Case

The dust FLRW limit is  $M = M_0 r^3$ ,  $f = -kr^2$ ,  $a = 0$ ,  $R = rS(t)$ , and the  $R = 2M$  locus is given by

$$S(t_{AH}) = 2M_0 r^2 \quad (295)$$

In the collapse phase of a  $k = +1$  model, the time of the future AH is

$$\cos \eta_{AH} = 1 - 2r^2 \quad (296)$$

$$\rightarrow t_{AH} = M_0 \left[ \pi + \arccos(2r^2 - 1) + 2r\sqrt{1 - r^2} \right] \quad (297)$$

which has slope

$$\left(\frac{dt}{dr}\right)_{AH} = -\frac{4M_0r^2}{\sqrt{1-r^2}} \quad (298)$$

while the light rays have slopes

$$\left(\frac{dt}{dr}\right)_n = \pm\frac{S}{\sqrt{1-r^2}} = \pm\frac{2M_0r^2}{\sqrt{1-r^2}} \quad (299)$$

Clearly the future AH is incoming timelike. The result extends to all  $k$  values, and the converse holds for the past AH in the expansion phase.

## Behaviour Near the Bang or Crunch

Consider eq (194) for the locus of the future AH in a collapsing elliptic region,  $f < 0$ ,  $\pi < \eta \leq 2\pi$ , in terms of parameter  $\eta$ . Near the crunch,  $\bar{\eta} = 2\pi - \eta \rightarrow 0$ , we find

$$\begin{aligned} 0 = & \left[ 1 - \sqrt{\frac{(-f)}{(1+f)}} \left(\frac{2}{\bar{\eta}}\right) \right] \left\{ \frac{(-f)^{3/2}a'}{M} \left(\frac{4}{\bar{\eta}^3}\right) - \frac{f'}{f} \left(\frac{12\pi}{\bar{\eta}^3}\right) + \frac{M'}{M} \left(\frac{8\pi}{\bar{\eta}^3}\right) \right\} \\ & + \left[ \sqrt{\frac{(-f)}{(1+f)}} \left(\frac{2}{\bar{\eta}}\right) \right] \frac{E'}{E}. \end{aligned} \quad (300)$$

As noted previously, when  $E' = 0$ , the solution makes the first bracket zero,  $\bar{\eta} \approx 2\sqrt{-f} \rightarrow 0$ . (Even in this case, where we know  $R = 2M$  is the AH, the fact that  $R'$  diverges at  $R = 0$  means we must multiply through by  $\bar{\eta}$  to make the rhs zero there.) Notice too that the no shell crossing condition (126) ensures the second bracket is generically non-negative where  $M' > 0$  and non-positive where  $M' < 0$ . Assuming we aren't near an origin,  $0 < M < \infty$ , it is clear that, even if  $f \rightarrow 0$ , the last two terms in this second bracket are divergent, with the middle one dominant, making the  $E'$  term negligible. Thus  $\bar{\eta} \approx 2\sqrt{-f}$  is still the solution in the limit. However (12) in the  $\bar{\eta} \approx 2\sqrt{-f} \rightarrow 0$  limit shows that the time from AH to crunch goes to

$$b - t_{AH} \rightarrow \frac{M}{(-f)^{3/2}} \frac{\bar{\eta}^3}{6} \rightarrow \frac{4M}{3} \quad (301)$$

where the crunch time  $b(r)$  is defined in (128). Therefore the future AH does not intersect the crunch away from an origin. The result is just the time reverse for the past AH near the bang in an expanding region, and a similar calculation applies for hyperbolic or extended parabolic regions, giving the same result.

An  $f = 0$  locus is where an interior elliptic region joins to an exterior hyperbolic or parabolic region. The transition involves the lifetime of the worldlines diverging, so either the crunch goes to the infinite future, or the bang goes to the infinite past. Since there is only one AH in a hyperbolic or parabolic region, one of the two AH loci in the elliptic region also exits to infinity before  $f = 0$  is reached.

A third possibility where  $f$  is only asymptotically zero (the asymptotically flat case) is that both the bang and the crunch diverge to the infinite past and future, and the two AHs go with them.

## Behaviour Near an Origin

Consider eq (194) again. Near a regular origin, along a constant  $t$  or constant  $\eta$  surface (see section 4),  $M \approx \mu(-f)^{3/2}$ ,  $E \approx \nu(-f)^{n/2}$  for some positive constants  $\mu$  &  $\nu$ , and  $f \rightarrow 0$ , so that

$$0 = \left[ 1 + \sqrt{-f} \frac{\sin \eta}{(1 - \cos \eta)} \right] \left\{ -\frac{a'}{\mu} \left( \frac{\sin \eta}{(1 - \cos \eta)^2} \right) + \frac{f'}{2f} \right\} - \left[ \sqrt{-f} \frac{\sin \eta}{(1 - \cos \eta)} \right] \frac{nf'}{2f} \quad (302)$$

We divide through by  $f'$  and define  $X = -\sqrt{-f} \frac{\sin \eta}{(1 - \cos \eta)}$  which is positive for  $\eta > \pi$ , giving

$$0 = [1 - X] \left\{ -\frac{a'}{\mu f'} \left( \frac{\sin \eta}{(1 - \cos \eta)^2} \right) + \frac{1}{2f} + \frac{X}{1 - X} \frac{n}{2f} \right\} \quad (303)$$

Though  $a'$  and  $M'$  always have opposite signs,  $f'$  may have either sign in an elliptic region, but in general we don't expect terms to cancel in the curly brackets. Thus, whether or not the  $a'$  term diverges, we must have  $X \rightarrow 1$ , i.e.  $\sin \eta \rightarrow 0$  so that

$$\bar{\eta} = 2\pi - \eta \rightarrow 2\sqrt{-f} \quad (304)$$

Unlike the previous case, though,  $M \rightarrow 0$  ensures the AH intersects the crunch here,

$$b - t_{AH} \rightarrow \mu \frac{\bar{\eta}^3}{6} \rightarrow 0 \quad (305)$$

As always, the time reverse applies in an expanding phase, and the hyperbolic and parabolic cases give the same result.